東海大学大学院平成 25 年度博士論文

Anti-Tn-antigen MLS128 monoclonal antibody: Its effects on colon cancer cells and characterization and identification of its receptor

指導　　山口陽子　教授

東海大学大学院総合理工学研究科
総合理工学専攻

NORMAIZA BINTI ZAMRI

TABLE OF CONTENTS

Abbreviations

mAb	monoclonal antibody
GP	glycoprotein
IGF	insulin-like growth factor
R	receptor
EGF	epidermal growth factor
FBS	fetal bovine serum
SFM	serum-free medium
SDS	sodium dodecyl sulfate
PAGE	polyacrylamide gel electrophoresis
PVDF	polyvinylidene difluoride
HRP	horseradish peroxidase
BSA	bovine serum albumin
IB	immunoblotting
IP	immunoprecipitation
SFK	Src family kinase
MAPK	mitogen-activated protein kinase
Tyr	tyrosine
IRS1	insulin receptor substrate 1
AKT	protein kinase

Chapter 1

INTRODUCTION

1.1 Tn antigen

The colonic epithelium secretes mucus, and this mucus consists mainly of mucin glycoproteins, or mucins. Mucins are a family of high-molecular-weight, heavily glycosylated proteins that facilitate cell signaling and the formation of chemical barriers. Mucins contain *O*-linked oligosaccharides synthesized on a polypeptide backbone. The most abundant form of *O*-glycosylation (termed mucin-type) is characterized by a α-N-acetylgalactosamine (GalNAc) attached to the hydroxyl group of Ser/Thr side chains (Springer *et al*., 1995, Itzkowitz *et al.,* 1992, Springer *et al.,* 1997). A schematic presentation of secreted and membrane-bound mucin-type O-linked glycan is shown in Fig. 1.

Figure 2 shows a schematic diagram of glycosylation in the O-linked pathway. In tumor cells, the glycoproteins are often abnormal, both in structure and quantity. Incomplete glycosylation is a frequent event of glycosylation alterations in cancer cells. This results in the appearance of precursor structures that would remain cryptic or masked in normal cells because of further glycosylation. Compared to O-glycans from normal mucins, cancer-associated *O*-glycans can be highly sialylated and less sulfated; they are often truncated and often contain Tn antigen and its sialylated forms.

In the normal epidermis and benign tumors of that tissue, Tn antigens are generally masked by covalently linked carbohydrates whereas in most primary and epithelial malignant tumors deficient glycosyltransferase or increased glycosidase activity leads to their exposure. This makes the Tn antigen a sensitive and specific marker for carcinoma detection and for monitoring treatment during and after cancer therapies.

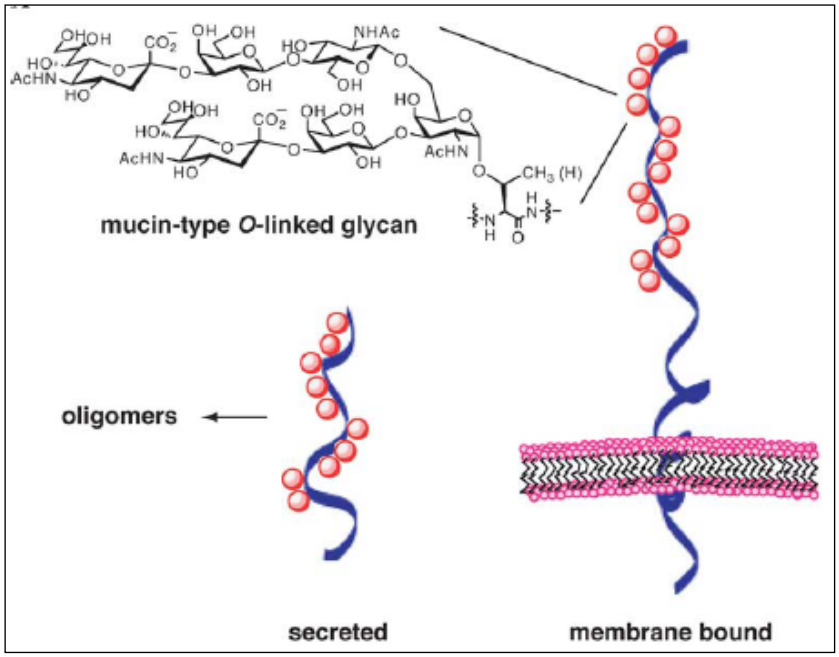

Figure 1. Mucin-type O-linked glycosylation. Architecture of membrane-bound and secreted mucins that crosslink into oligomers. Blue ribbons represent protein backbones. Red circles represent O-linked glycans. (Hang *et al*., 2005)

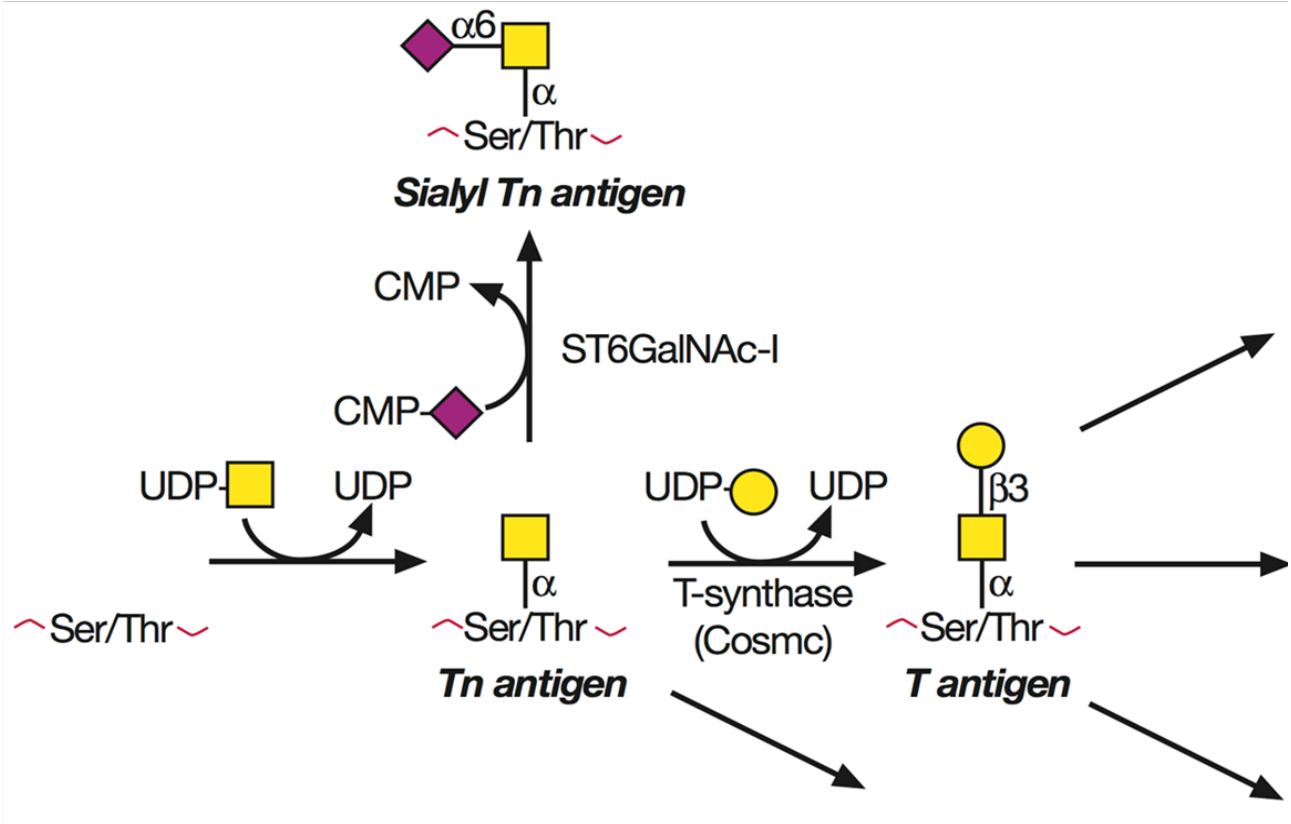

Figure 2. A schematic diagram of glycosylation in the O-linked pathway.
(Varki *et al*. eds., 2009, Chapter 44, Fig. 3)

The Tn antigen was detected in about 90% of human carcinomas, a finding that attracted attention in the field of oncology (Springer *et al.,* 1984, 1995, 1997). Tn antigen has thus been thoroughly studied for decades as a cancer biomarker and was thus characterized as one of the most specific structures associated with human cancer (Charpin *et al.,* 1992, Takahashi *et al.,* 1988). Recent studies, however, have shifted to the potential targeting of Tn antigen for cancer therapeutics (Reis *et al.,* 1998, Oppezzo *et al*., 2000, Ando *et al*., 2008, Kubota *et al*., 2010, Welinder *et al.,* 2011). One example is the anti-Tn mAb 83D4, produced by a murine hybridoma generated by immunization with a cell suspension from a paraffin block of human breast carcinoma tissue (Pacino *et al.,* 1990, Charpin *et al.,* 1992). Another example is GOD3-2C4, which was generated through somatic cell hybridization after immunization of a mouse with a tumor cell line and a Tn carrying mucin (Welinder *et al*., 2011). As listed in Table 1, various anti-Tn-antigen monoclonal antibodies (mAbs) have been produced in the past. Although most anti-Tn-antigen mAbs are IgM, as is expected for anti-carbohydrate monoclonal antibodies, the MLS128 mAb that

was used in the current study is IgG_3.

MONOCLONAL ANTIBODIES

Name	Raised against	Isotype	Reference
NCC-LU-81	Lung carcinoma cell line	IgM	97
FBT3	Tn positive erythrocytes	IgM	98
164H.1	Human serum albumin-GalNAc	IgM	99
CU-1	Lung carcinoma cell line	IgG_3	100
6E6-H5-G9	Tn positive erythrocytes	IgM	101
Etn 1.01	Tn positive erythrocytes	IgM	102
MLS128	Colorectal carcinoma cell line	IgG_3	103
91S8	Colorectal carcinoma cell line	IgM	104
5F4	Asialo-OSM	IgM	105
83D4	human breast tumour	IgM	106
PMH1	MUC2-GalNAc	IgM	75

PLANT LECTINS

Name	Specificity	Reference
Isolectin B4 from *Vicia villosa*	Tn	107
Salvia sclarea	Tn	108
isolectin A4 from *Griffonia simplicifolia* lectin-I	Tn	74
Moluccella laevis	Tn > sialyl-Tn, A, N	109

Table 1. List of monoclonal antibodies and lectins with Tn antigen-binding activity.

(Freire *et al.,* 2003)

1.2 MLS128

MLS128 was derived from a mouse immunized with LS180 human colon carcinoma cells (Numata *et al*., 1990). It is a Tn-specific monoclonal antibody (mAb) that binds to carbohydrate epitopes consisting of two or three consecutive Tn antigens (Nakada *et al*., 1991, 1993, Osinaga *et al*., 2000). Schematic representations of Tn and T antigens as well as two or three consecutive Tn antigens (Tn2 and Tn3, respectively) are shown in Fig. 3A-D (Fujita-Yamaguchi, 2013). The current study investigated the therapeutic potential of anti-Tn-antigen antibodies using MLS128. MLS128 binds to a 110 kDa glycoprotein (GP) on the surface of colon cancer cells (Morita *et al*., 2009, Zamri *et al*., 2012), as shown in Fig. 3E.

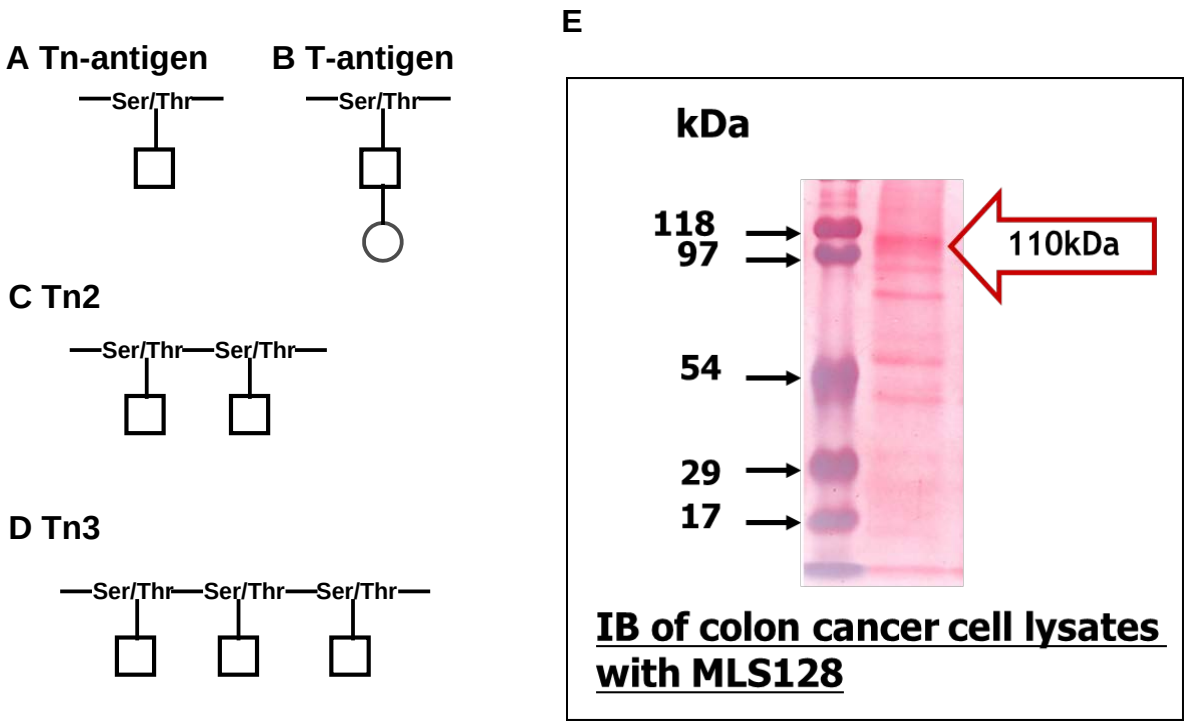

Figure 3. Schematic representation of Tn and T antigens (A-D) and immunoblotting (IB) of colon cancer cell lysates with MLS128 (E). In A-D, square and circle represent N-acetyl galactosamine and galactose, respectively. Incomplete glycosylation in the O-linked pathway results in expression of the Tn antigen (A) or the T antigen (Thomsen–Friedenreich antigen or unmodified core 1 structure) (B). Two or three consecutive Tn-antigen-peptides that were used to determine kinetic parameters for MLS128 and 83D4 (Osinaga *et al.,* 2000, Matsumoto-Takasaki *et al*., 2012) are shown in C and D.

MLS128 is IgG_3 that recognizes the structure of two or three consecutively arranged GalNAc of Tn antigens (Nakada *et al.,* 1991, 1993). Osinaga *et al.* used surface plasmon resonance (SPR) to measure the kinetic parameters for anti-Tn-antigen 83D4 and MLS128, and they showed that MLS128 binds to a synthetic glycopeptide, Tn3, with approximately 10 times greater affinity than that for Tn2, whereas 83D4 binds to both glycopeptides with a similar level of affinity (Osinaga *et al.,* 2000). Recent efforts have focused on molecular cloning of the variable domains of MLS128 (Yuasa *et al.,* 2012) and determining the thermodynamic properties of Tn3's affinity for MLS128 (Matsumoto-Takasaki *et al.,* 2012).

Previous studies demonstrated that MLS128 inhibits the growth of LS180 and HT29 colon cancer cells and MCF7 breast cancer cells. Down-regulation of insulin-like growth factor-I receptor (IGF-IR) signaling was suggested as one possible mechanism for the inhibitory action in LS180 colon cancer cells (Morita *et al*., 2009).

Based on previous findings of Morita *et al*., the effects of MLS128 on three colon cancer cell lines and MLS128's mechanisms of action, including a possible association with IGF-IR signaling pathways, were investigated (Chapter 2, Zamri *et al*., 2012). Chapter 2 also describes significant findings, namely that the growth of LS180, LS174T, and HT29 human colon cancer cells is in part dependent on IGF-IR signaling and that down-regulation of IGF-IR plays a role in the inhibition of colon cancer cell growth via 1H7 (anti-IGF-IR mAb).

1.3 Molecularly targeted therapy

Molecularly targeted cancer therapies utilize drugs or other substances that block the growth and spread of cancer by interfering with specific molecules involved in tumor growth and progression. By focusing on molecular and cellular changes that are specific to cancer, molecularly targeted cancer therapies are more effective than other types of treatments such as chemotherapy and radiotherapy since they are less harmful to normal cells (Claus-Henning and Heinz-Josef, 2009).

Molecularly targeted cancer therapies can interfere with cancer cell division (proliferation) and spread via different molecular mechanisms. By specifically blocking signals that lead to uncontrolled cancer cell growth and division, molecularly targeted cancer therapies can help stop the progression of cancer and they may induce cancer cell death through apoptosis. Other molecularly targeted therapies can cause cancer cell death directly, by specifically inducing apoptosis, or indirectly by stimulating the immune system to recognize and destroy cancer cells and/or by delivering toxic substances directly to the cancer cells.

Once a target has been identified, a molecularly targeted therapy can be developed. Most molecularly targeted therapies are either small-molecule drugs or mAbs. Small-molecule drugs are typically able to diffuse into cells and can act on targets that are found inside the cell. Most mAbs cannot penetrate the cell's plasma membrane and are directed against targets that are outside cells or on the cell surface.

A number of molecularly targeted cancer therapies have been approved by the US Food and Drug Administration (FDA) for the treatment of specific types of cancer. Others are being studied in clinical trials and many more are in preclinical testing.

1.4 The insulin-like growth factor I receptor and cell signaling

The insulin-like growth factor I receptor (IGF-IR) is a tyrosine kinase cell-surface receptor activated by its ligand, either IGF-I or IGF-II (Fig. 4). IGF-IR controls the proliferation of cells in a variety of ways (Butler *et al.*, 1998, Valentinis and Baserga, 2001), namely:

1) It sends a mitogenic signal.
2) It protects cells from a variety of apoptotic injuries.
3) It promotes the growth of cell size (a requirement for cell division).
4) It plays a crucial role in the establishment and maintenance of the transformed phenotype.
5) It regulates cell adhesion and cell motility.
6) It can induce terminal differentiation.

IGF-IR is expressed in most cell types, the only known exceptions being hepatocytes and mature B cells. Because IGF-IR is found ubiquitously, it plays a role in regulating the growth of many cell types even though the primary growth factor might be another molecule. IGF-I is thus often called a “survival factor.”

Some cancer cells depend on the function of specific molecules for their growth, survival, and metastatic potential. Targeting of these molecules has arguably been the best therapy for cancer, as demonstrated by the success of tamoxifen and trastuzumab in treating breast cancer (Yee, 2006). IGF-IR has also been studied as a potential target for cancer therapy. Many drugs and methods have been used to inhibit or disrupt IGF-IR signaling pathways (Yee, 2006). However, one major drawback of this approach is that are numerous potential toxicities associated with disruption of IGF-IR activation in normal tissues.

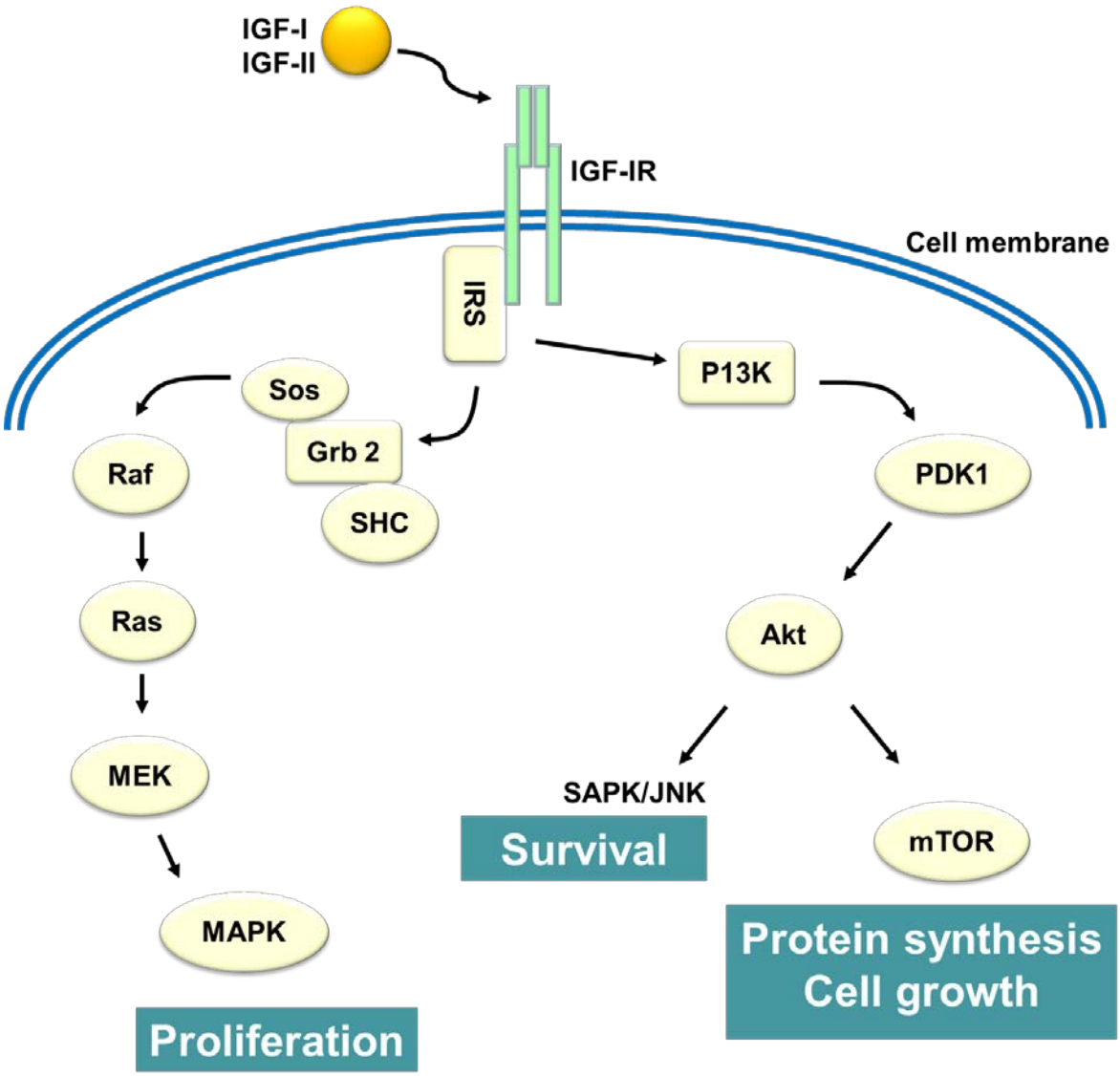

Figure 4. Diagram of the insulin-like growth factor 1 receptor (IGF-IR) pathway.

By binding to its ligand, IGF-IR activates receptor tyrosine kinases and it activates two key signal-transduction components: the GTPase Ras-Raf-ERK/MAPK pathway and; the lipid kinase PI3K/AKT pathway. RAS activates Raf, which phosphorylates ERK/MAPK (MEK) kinases and stimulates cell proliferation. AKT controls cell survival, the cell cycle, cell growth, and metabolism through phosphorylation of a number of key substrates such as mTOR.

1.5 Background

A previous study (Morita *et al.,* 2009) described the therapeutic potential of tumor-associated carbohydrate antigen-specific antibody, that is, the effects of MLS128 on LS180 and HT29 colon cancer cells and MCF-7 breast cancer cells.

The study indicated that:

1.5.1. MLS128 inhibits colon and breast cancer cell growth, as shown in Fig. 5.

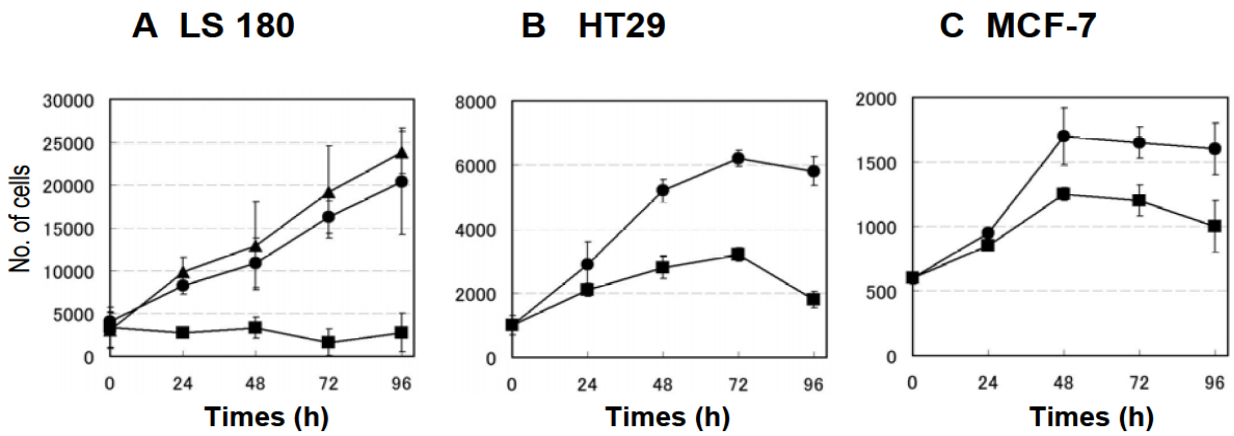

Figure 5. Effects of MLS128 on the growth of LS180 and HT29 human colon cancer cells and MCF-7 breast cancer cells.
Time course of cancer cell growth with 25 μg/mL of MLS128(■), 25 μg/mL of control IgG3 (▲), or PBS(●)

(Morita *et al.,* 2009)

1.5.2. FACS confirmed that MLS128 binds to the cell surface of various cell lines, as shown in Fig. 6.

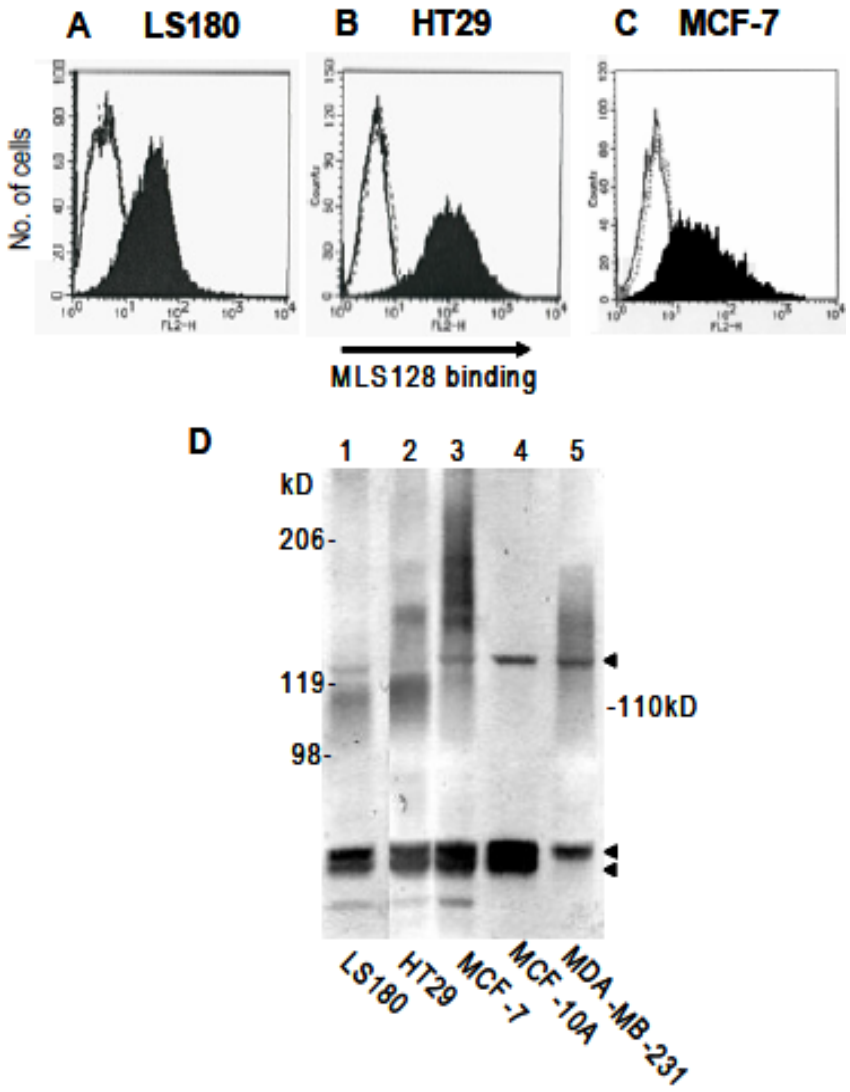

Figure 6. **Binding of MLS128 to cancer cells or solubilized glycoproteins.** MLS128 binding to LS180 (**A**), HT-29 (**B**), and MCF-7 (**C**) cancer cells was measured with FACS. In **D**, solubilized plasma membranes prepared from various cancer cell lines, *i.e.* LS180 (lane 1), HT-29 (lane 2), MCF-7 (lane 3), MCF-10A (lane 4), and MDA-MB-231 (lane 5), were subjected to SDS-PAGE and IB with MLS128, as described in the Materials and Methods. Molecular markers and the 110 kDa GP are indicated. The 125, 75, and 73 kDa proteins marked with a triangle (◄) are endogenous biotin-containing enzymes.

(Morita *et al.,* 2009)

1.5.3. MLS128 treatment of LS180 colon cancer cells caused down-regulation of IGF-IR and epidermal growth factor receptor (EGFR), as shown in Fig.6.

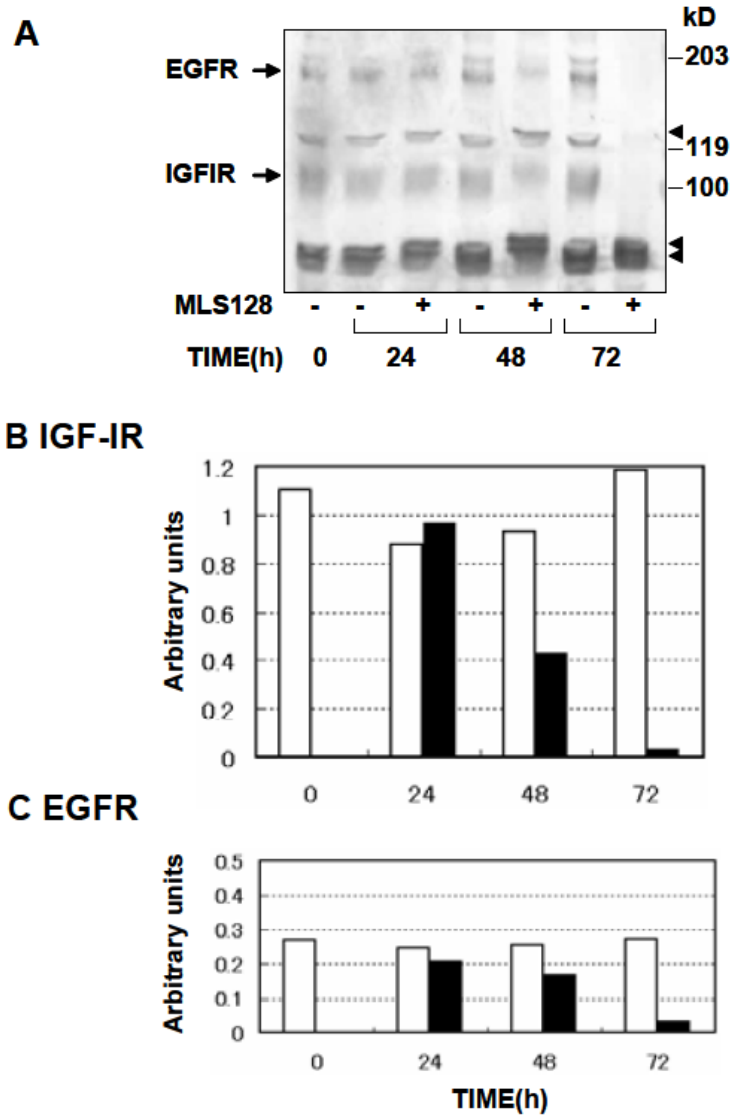

Figure 7-1. Down-regulation of IGFIR and EGFR in LS180 cells after MLS128 treatment.

LS180 cells were treated with MLS128 (25 μg/mL) for the times indicated. Cell lysates were prepared from live cells and subjected to SDS-PAGE followed by IB with anti-IGFIR β subunit antibody and anti-EGFR. The 125, 75, and 73 kDa proteins marked with a triangle (◄) are endogenous biotin-containing enzymes. The amounts of IGFIR β subunits (B) and EGFR (C) after PBS (□) or MLS128 (■) treatment were estimated using densitometric analysis with the 75 and 73 kDa biotin-containing enzymes (◄) as internal controls. (Morita *et al*., 2009)

1.5.4. Use of purified human IGF-IR revealed no cross-reactivity of MLS128 to IGFIR, as shown in Fig. 7-2.

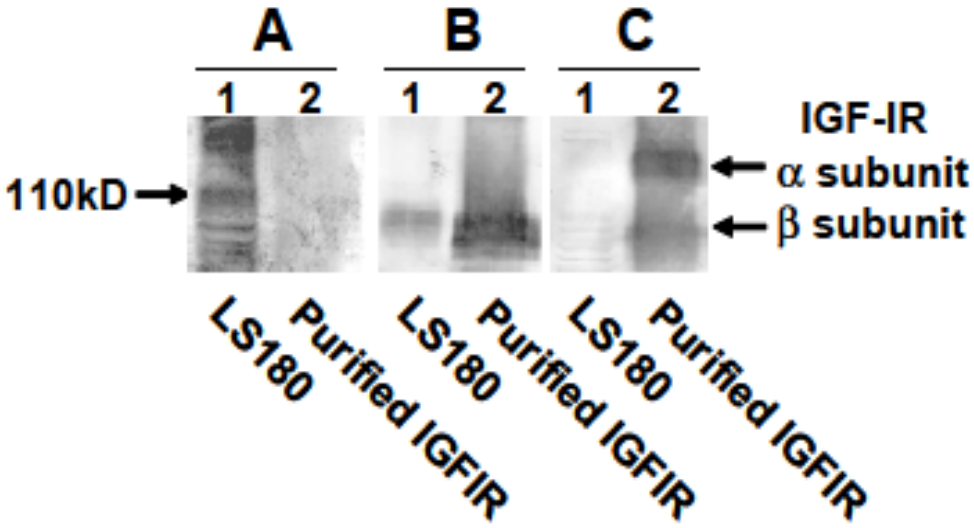

Figure 7-2. Cross-reactivity of MLS128 and IGF-IR.
LS180 cell lysates and purified human placental IGFIR were compared in triplicate by IB with MLS128 (**A**), anti-IGFIR β subunit polyclonal antibody (**B**), and IGFIR-crossreactive anti-IR polyclonal antibody (**C**). The positions of the IGFIR α and β subunits as well as the 110-kDa MLS128-reactive GP are indicated with arrows.

(Morita *et al*., 2009)

1.6. Proposed working hypothesis and the aims of the studies conducted

Based on the findings of Morita *et al.* (2009) as described earlier, the current study proposed a working hypothesis as shown in the diagram below (Fig. 8).

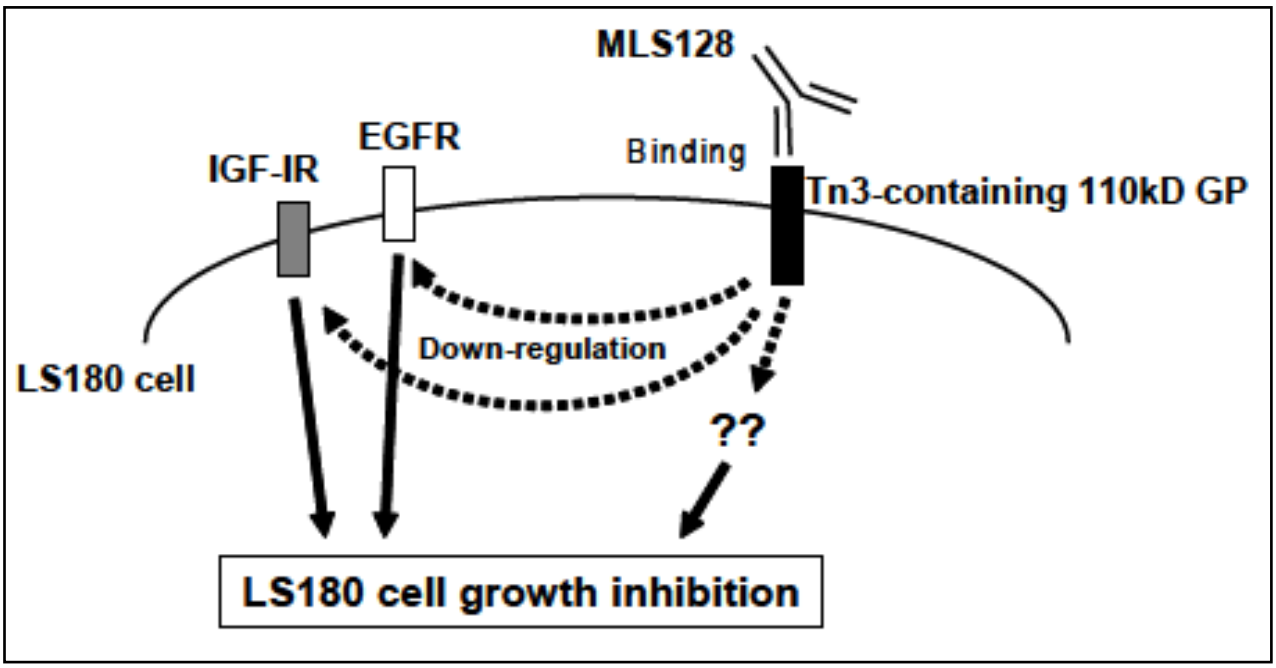

Figure 8. MLS128-induced inhibition of LS180 cell growth (Morita *et al*., 2009**)**.

By binding to the 110 kDa GP on the cell surface of LS180 colon cancer cells, MLS128 inhibits growth - at least in part - through IGF-IR and EGFR down-regulation via as-yet-unknown mechanisms.

The aims of this study were to investigate and understand the inhibitory action of MLS128 and to characterize and identify the MLS128 cell surface-binding protein 110 kDa GP.

Chapter 2

Effects of two monoclonal antibodies, MLS128 against Tn antigen and 1H7 against IGF-IR, on the growth of colon cancer cells

2.1 Summary

Drawing on the hypothesis proposed earlier, this chapter discusses the role of IGF-IR signalling in the growth of colon cancer cells and its possible interaction with MLS128-induced inhibition of cell growth. Three colon cancer cell lines were used (LS180, LS174T and HT29 human colon cancer cells) to investigate the effects of MLS128 and anti-IGF-IR antibody 1H7 on cell growth.

Both MLS128 and 1H7 treatment significantly inhibited the growth of colon cancer cells. All three colon cancer cell lines expressed IGF-IR. Their growth was in part IGF-I dependent, but inhibition by MLS128 was independent of IGF-IR signalling. All of the colon cancer cell lines expressed a 110 kDa GP for MLS128 binding.

1H7 treatment caused down-regulation of IGF-IR but did not affect 110 kDa GP levels. MLS128 treatments resulted in partial disappearance of the 110kDa band but did not affect IGF-IR levels.

Western blot analyses of colon and breast cancer cell lysates revealed that colon and breast cancer cells differed significantly in patterns of expression of growth-related molecules while colon cancer cells had similar but distinctive patterns of expression.

In conclusion, MLS128 inhibited the growth of colon cancer cells by binding to the 110 kDa GP receptor. Inhibition of growth by MLS128 did not appear to affect IGF-IR signalling and instead only affected other growth signalling pathways.

2.2 Introduction

This study focused on the role of IGF-IR signalling in the growth of colon cancer cells and its possible interaction with MLS128-induced inhibition of cancer cell growth.

IGF-IR signalling is known to play an important role in proliferation, anti-apoptosis, and differentiation. IGF-I and II bind to IGF-IR with a high affinity and thus activate IGF-IR tyrosine-kinase, which in turn stimulates downstream signalling cascades. Increased IGF-IR signalling has been reported to contribute to cancer cell growth and development. IGF-IR is thus an important target for cancer treatment (LeRoith *et al*., 1995, Baserga *et al.,* 1997, Pollak *et al*., 2004, Larsson *et al*., 2005, Miller *et al.,* 2005). Anti-IGF-IR mAb 1H7 (Li *et al*., 1993, 2000, Sachdev *et al*., 2003, Ye *et al*., 2003) was used in the current study for comparison to MLS128.

One cannot reasonably assume, however, that the growth of colon cancer cells depends solely on IGF-IR signalling. In fact, the current study revealed that addition of anti-IGF-IR mAb 1H7 significantly inhibited cell growth of all of the colon cancer cell lines studied, but this inhibition amounted to approximately 60%. Individual cancer cells are likely to be equipped with diverse growth signalling pathways, and one or two particular signalling pathways may play a major role in the growth of a particular cancer cell line. Expression of several possible growth-related surface molecules has thus been measured in three colon cancer cell lines to ascertain different mechanisms that might play a role in the growth of colon cancer cells. Western blot analyses of colon and breast cancer cells differ significantly with regard to their patterns of expression of growth-related molecules. Although three colon cancer cell lines expressed molecules in the same patterns, all three were distinctive.

In summary, this study demonstrated that 1H7 and MLS128 inhibited the growth of colon cancer cells. Colon cancer cells were in part dependent on IGF-IR signalling. Inhibition of growth by MLS128 does not however, apparently depend on IGF-IR signalling, suggesting that MLS128 likely inhibits the growth of colon cancer cells by affecting other growth signalling pathways.

2.3 Materials

Production and characterization of MLS128 (anti-Tn antigen IgG_3) mAb were as previously described (Numata *et al.* 1990, Nakada *et al.* 1991, 1993).

Production and characterization of 1H7 (anti-IGF-IR IgG_1) mAb were as previously described (Li *et al.* 1993).

LS180, LS174T, and HT29 human colon adenocarcinoma cells were obtained from the American Tissue Type Culture Collection.

Mouse anti-actin clone C4 antibody was obtained from MP Biomedicals, LLC. (Santa Ana, CA, USA).

Rabbit anti-IGF-IRβ, anti-EGFR mAb, rabbit anti-phospho-p44/42 MAPK (Thr202/Tyr204), rabbit anti-phospho Akt (Ser473) (193H12), rabbit anti-p44/42 MAPK, rabbit anti-CD44, anti-phosphotyrosine mAb, and rabbit anti-β actin were purchased from Cell Signaling Technology (Beverly, MA, USA).

Rabbit anti-c-Met and anti-E-cadherin antibodies were from Santa Cruz Biotechnology (Santa Cruz, CA. USA).

Anti-rabbit or –mouse secondary antibody labelled with biotin was from Kirkegaard & Perry Laboratories (Gaithersburg, MD, USA).

IGF-I was obtained from Sigma-Aldrich Biotechnology (St. Louis, MO, USA). Cell culture media (DMEM and McCoy's 5A) were purchased from Invitrogen (Carlsbad, CA, USA)

2.4 Methods

Cell Culture

LS180 and LS174T cells were cultured in DMEM containing 10% fetal bovine serum (FBS) supplemented with 4.5 mg/mL D-glucose and 110 µg/mL pyruvic acid. HT29 cells were cultured in McCoy's 5A containing 10% FBS. All culture media included a 1% penicillin-streptomycin solution (Sigma-Aldrich, St. Louis, MO, USA).

Effects of 1H7 or MLS128 on the growth of colon cancer cells

Cells (1×10^4) were plated in wells of a 96-well plate and cultured in 100µL of fresh media containing 10% FBS for 24 h. Attached cells were then washed twice with PBS and cultured in 100 µL of media containing 1% FBS in the presence or absence of MLS128 (25 µg/mL) or 1H7 (0.36 µg/mL). After culturing for 72 h, cells were collected from each well by treatment with trypsin-EDTA (Sigma-Aldrich). Live cell numbers were counted using a hemacytometer. Quadruple wells were prepared for each data point.

Effects of IGF on the growth of colon cancer cells

To measure the effects of IGF-I on the growth of colon cancer cells, cells (5×10^3) were plated in wells of a 96- well plate and cultured in 100 µL of respective medium containing 10% FBS for 24 h. Attached cells were washed twice with PBS and serum-deprived for 24 h in regular growth medium containing 0.1 % BSA instead of FBS (SFM). Medium was replaced with SFM containing 0, 0.76, or 76 ng/mL of IGF-I. After culturing for 24, 48, and 72 h, cell growth was determined using a CCK-8 cell counting kit (Dojindo, Kumamoto, Japan) in accordance with the manufacturer's instructions. Absorbance at 450 nm was measured with a plate reader (Bio-Rad, Hercules, CA, USA). Quadruple wells were prepared for each data point.

Western blot analyses of various growth-related proteins in colon and breast cancer cells

LS180, LS174T, and HT-29 colon cancer cells as well as MCF-7 breast cancer cells were cultured in their respective media. Cells were collected by scraping and then centrifuged at 200 × g for 5 min. Cells were solubilized in 50 mM Tris-HCl buffer, pH 7.4, containing 1% NP40, 2 mM EDTA, 100 mM NaCl, 10 mM sodium orthovanadate, 1 mM PMSF, and protease inhibitors (lysis buffer) on ice for 15 min. Supernatants were obtained from solubilized cells by centrifugation at 17,000 × g for 10 min. Protein concentrations were measured using the Bradford method. The solubilized proteins (5 and 25 μg) from each cell line were separated by sodium dodecyl sulfate-polyacrylamide gel electrophoresis (SDS-PAGE) and transferred to PVDF membranes. The membrane was blocked with 3% BSA in 50 mM Tris-HCl buffer, pH 7.4, containing 0.15 M NaCl and 1% Tween 20 (TBST) for 1 h at room temperature. Western blotting was carried out with anti-IGF-IR, MLS128, anti-EGFR, anti-c-Met, anti-E-cadherin, and anti-CD44 antibodies as primary antibodies. Bound primary antibodies were then detected with biotin-labeled secondary antibodies using a Vectastain ABC-Amp kit and an alkaline phosphatase kit (Vector Laboratories, Inc. Burlingame, CA, USA). Alternatively, bound primary antibodies were detected with HRP-conjugated secondary antibodies and color development using Ez West blue (ATTO Co., Tokyo, Japan). The blots were analyzed using the NIH Image 1.63 Analysis system (Research Service Branch, the National Institute of Mental Health, USA).

Effects of 1H7 or MLS128 treatment on IGF-IR and 110 kDa GP levels in colon cancer cell lines according to Western blot analyses

LS180, LS174T, and HT29 colon cancer cells (8×10^5) were cultured in respective media containing 10% FBS for 24 h in wells of 6-well plates. Cells were then cultured in the respective media containing 1% FBS in the presence or absence of MLS128 (25 μg/mL) or 1H7 (0.36 μg/mL). After culturing for 24, 48, and 72 h, cells were collected and solubilized in 50 μL of the lysis buffer as described above. The solubilized proteins (2 μg per lane) were separated by SDS-PAGE and transferred to PVDF membranes. The membranes were blocked with 3% BSA in TBST for 1 h at room temperature. After incubation with

primary antibodies against 110 kDa GP (MLS128), the IGF-IR β subunit, and β-actin for 16 h, bound primary antibodies were detected as described above.

Effects of MLS128 on IGF-IR signaling in colon cancer cells

Cells (8×10^5) were plated in wells of a 6-well plate and cultured in respective medium containing 10% FBS for 24 h. Cells were then cultured in SFM containing 0.1% BSA or 25 μg/mL of MLS128. 50 ng/mL of IGF-I was added to MLS128-treated and non-treated cells. After incubation for 5 or 10 min, cells were collected by centrifugation and subjected to solubilization in 50 μL of the lysis buffer for 15 min, followed by centrifugation at 17,000 × g for 10 min. Recovered supernatants containing solubilized proteins were assayed for protein concentrations. The solubilized proteins (5 μg per lane) were separated by SDS-PAGE and subjected to Western blotting as described above. Primary antibodies against p-Tyr, p-MAPK, and p-Akt were used for detection of IRS-1, MAPK, and Akt phosphorylation, respectively. After incubation at 4°C overnight, bound primary antibodies were detected using biotin-conjugated secondary antibodies and the Vectastain ABC-Amp kit (Vector Laboratories, Inc. Burlingame, CA, USA).

Statistical analyses

Levels of cell growth and Western blotted protein bands were expressed as means ± SE from 3 or more experiments. An unpaired Student's t-test was used to compare the growth or intensity of the bands in two groups of experiments performed in the absence and presence of mAb.

2.5 Results

2.5.1 Inhibition of the growth of three colon cancer cell lines by anti-Tn-antigen mAb or anti-IGF-IR mAb

A previous study (Morita *et al*., 2009) found that MLS128 inhibited the growth of LS180 and HT29 colon cancer cells as well as MCF-7 breast cancer cells. Thus, the current study compared MLS128's inhibition of the growth of the same two colon cancer cell lines and a third LS174T colon cancer cell line. Typical results for inhibition of the growth of LS180, LS174T, and HT29 colon cancer cells after 3 days of mAb treatment are shown in Fig. 9-1 A and B and Fig. 9-2 C, respectively. The mean ± SE from 3 or 4 experiments with each cancer cell line is summarized in Fig. 9-2 D.

MLS128 treatment of LS180, LS174T, and HT29 colon cancer cells for 3 days significantly inhibited cell growth (Fig. 9-1 A and B, and Fig. 9-2 C, respectively). Results confirmed previous findings that MLS128 inhibited the growth of LS180 and HT29 cells. In addition, inhibition of growth was also noted with the LS174T cell line, which is a variant of LS180 that had been maintained using trypsin in accordance with a subculture protocol. As shown in Fig. 9-2 D, 3 days of MLS128 treatment inhibited the growth of LS180, LS174T, and HT29 colon cancer cells by an average of 26%, 34%, and 18%, respectively.

Anti-IGF-IR 1H7 significantly inhibited the growth of LS180, LS174T, and HT29 colon cancer cell lines by 37%, 43%, and 30%, respectively (Fig. 9-2 D). An interesting finding is that monolayer growth of colon cancer cells was significantly inhibited by 1H7.

Monolayer MCF-7 cell growth, however, was not significantly inhibited in the presence of 1H7 scFv-Fc. The same is not true for breast cancer, since 1H7 scFv-Fc has been found to markedly inhibit anchorage- dependent MCF-7 cell growth in vitro and to markedly inhibit MSF-7 and T61 breast cancer tumor growth in vivo via down- regulation of IGF-IR. (Sachdev *et al*., 2003, Ye *et al*., 2003)

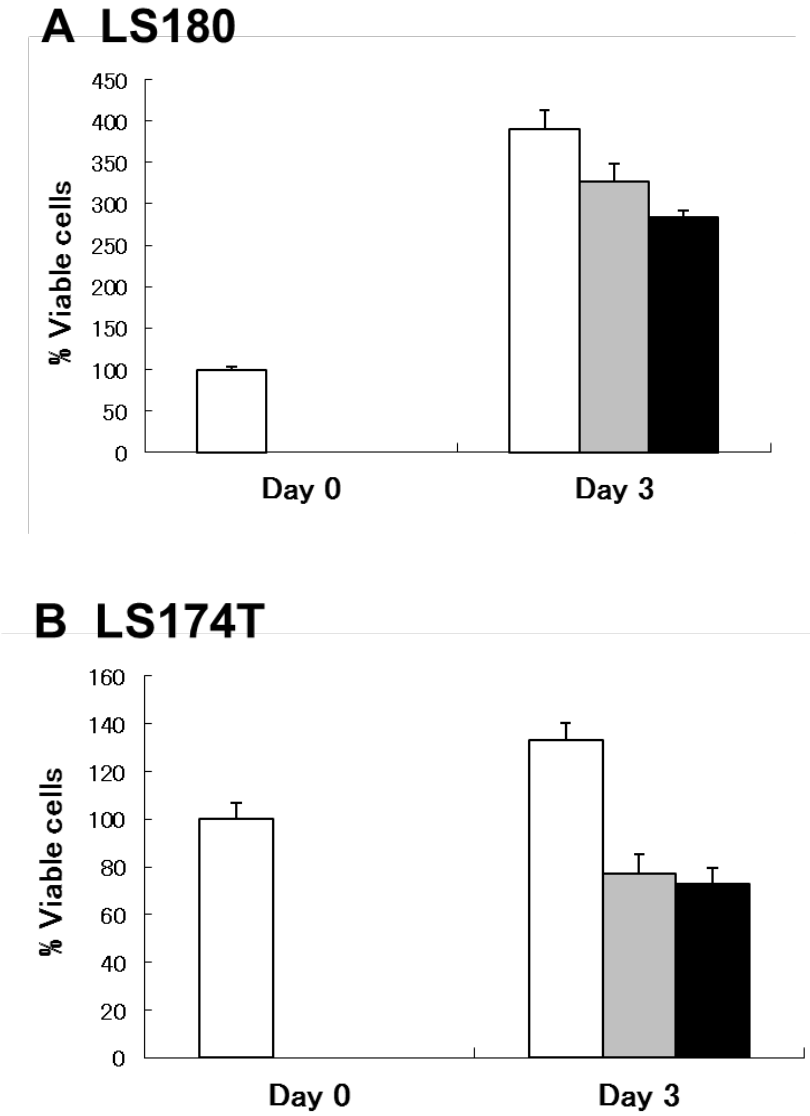

Figure 9-1. Addition of MLS128 or 1H7 inhibits growth of three colon cancer cell lines.

Inhibition of the growth of three colon cancer cell lines by MLS128 (grey bars) and anti-IGF-IR 1H7 (black bars) was compared to the control (white bars). Experiments were performed as described in the Methods. Typical results for growth of LS180 and LS174T colon cancer cells after 3 days of mAb treatment are shown in A and B, respectively.

C HT29

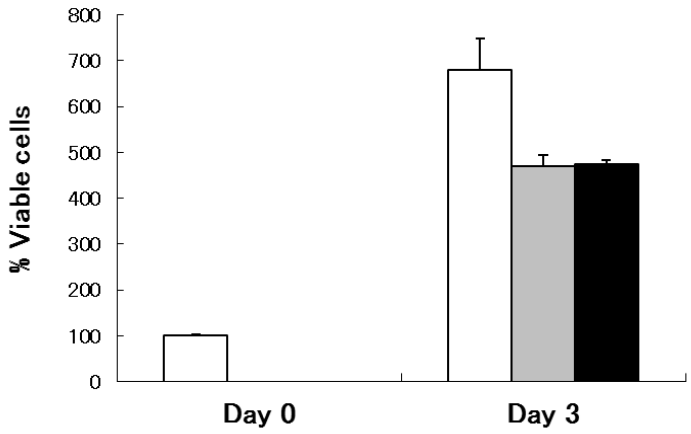

D

Relative cell growth (%) on Day 3 of three cell lines in the presence of MLS128 or 1H7 mAb

Colon cancer cells	MLS128	1H7
LS 180	73.7 ± 9.1 (n=3) p<0.05	63.0 ± 9.2 (n=3) p<0.05
LS174T	66.3 ± 11.0 (n=4) p<0.05	57.2 ± 9.9 (n=4) p<0.01
HT 29	81.8 ± 6.4 (n=3) p<0.05	70.5 ± 2.9 (n=3) p<0.01

Figure 9-2. Addition of MLS128 or 1H7 inhibits growth of three colon cancer cell lines.

Inhibition of the growth of three colon cancer cell lines by MLS128 (grey bars) and anti-IGF-IR 1H7 (black bars) was compared to the control (white bars). Experiments were performed as described in the Methods. Typical results for growth HT29 colon cancer cells after 3 days of mAb treatment are shown in C. The relative growth (% control), the average ± SE from 3 or 4 experiments for each cancer cell line, is summarized in D.

2.5.2 Examination of cell growth's dependence on IGF-I

LS180 (A), LS174T (B), and HT29 (C) cell growth were observed under serum-free conditions in the absence or presence of IGF-I.

The results shown in Fig. 10-1 and Fig. 10-2 indicate that the growth of three colon cancer cell lines is in part IGF-I-dependent. These results are consistent with the finding that anti-IGF-IR 1H7 inhibited the growth of all three colon cancer cell lines (Fig. 9-1 and Fig. 9-2) as previously noted.

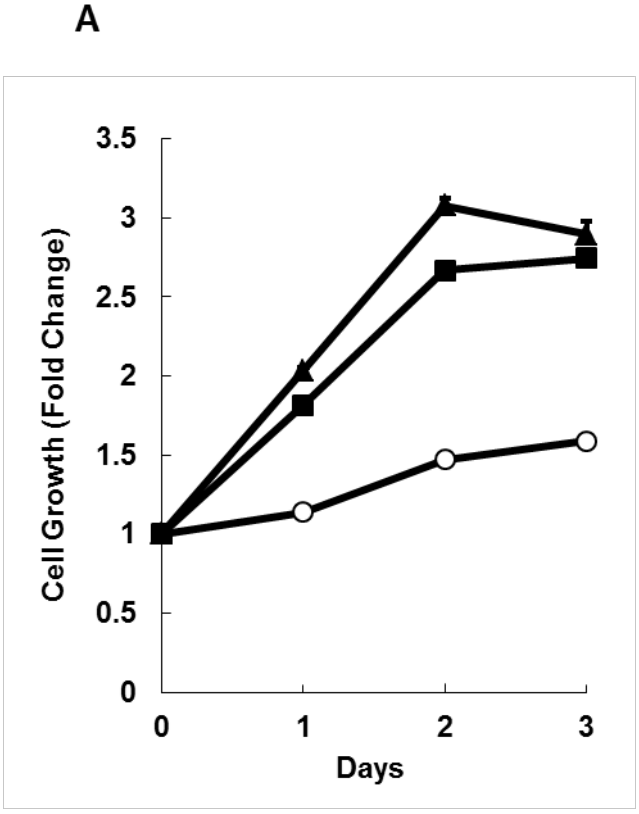

Figure 10-1. Growth of colon cancer cells is IGF-dependent.

LS180 cell growth was observed under serum- free conditions in the absence (○) or presence of 0.76 (■) or 76 ng/mL (▲) of IGF-I for 3 days as described in the Methods. Typical results from 2-4 experiments are shown.

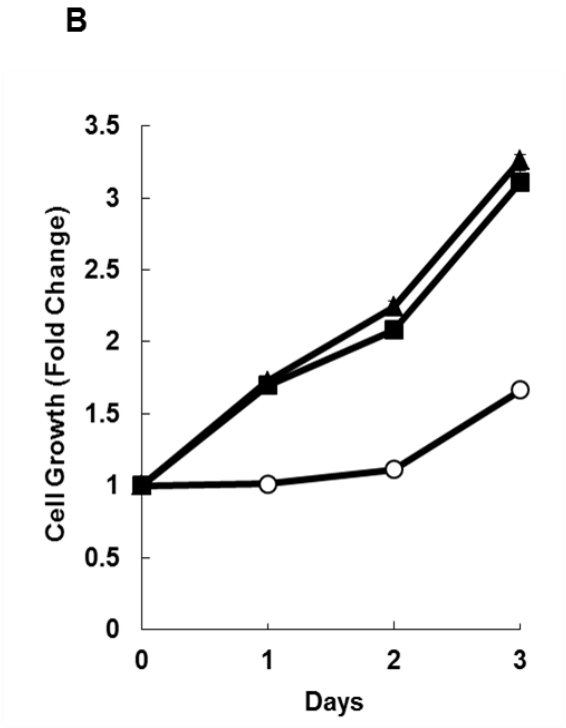

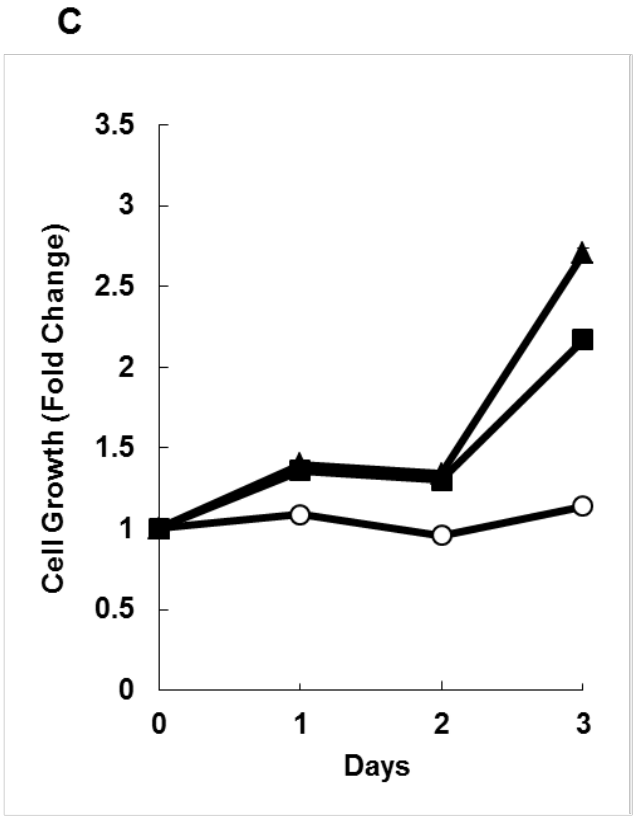

Figure 10-2. Growth of colon cancer cells is IGF-dependent.

LS174T (B), or HT29 (C) cell growth was observed under serum- free conditions in the absence (○) or presence of 0.76 (■) or 76 ng/mL (▲) of IGF-I for 3 days as described in the Methods. Typical results from 2-4 experiments are shown.

2.5.3 Effects of MLS128 on IGF-IR signaling

The effects of MLS128 on IGF-IR signaling were examined in three colon cancer cell lines. MLS128 did not affect the downstream signaling stimulated by IGF-I as indicated by IB of p-Tyr, p-MAPK, and p-Akt (Figs. 11, 12, and 13 for LS180, LS174T, and HT29 cells, respectively).

These results suggest that MLS128's inhibition of the growth of colon cancer cells is independent of IGF-IR signaling. While the effects of MLS128 on IGF-IR signaling were not obvious, MLS128 may affect basal phosphorylation of MAPK and Akt differently, in that MLS128 inhibited MAPK and Akt phosphorylation in LS180 cells, by 0.67 ± 0.04 (n = 3)- and 0.61 ± 0.22 (n = 3)- fold, respectively, but it activated IRS-1 and MAPK phosphorylation in HT29 cells by 1.21 ± 0.08 (n = 3)- and 1.25 ± 0.05 (n = 3)-fold, respectively.

These results indicate that MLS128 affects colon cancer cell signaling via as-yet-unidentified signaling pathways besides the IGF-IR signaling pathway.

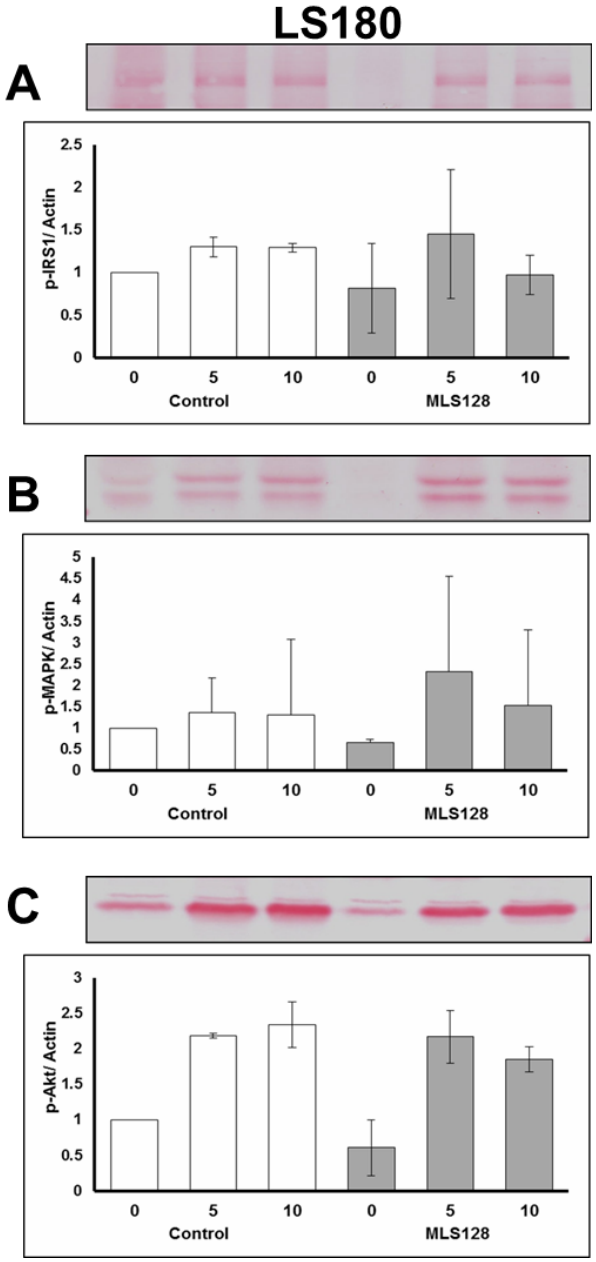

Figure 11. Effects of MLS128 on IGF-IR signaling in the LS180 colon cancer cell line. Briefly, 50 ng/mL of IGF-I was added to cells cultured in SFM containing 0.1% BSA (white bars) or 25 µg/mL of MLS128 (grey bars). After incubation for 5 or 10 min, cells were subjected to solubilization. The solubilized proteins (5 µg per lane) were separated by SDS-PAGE and subjected to Western blotting using primary antibodies against p-Tyr (A), p-MAPK (B), and p-Akt (C) for detection of IRS-1, MAPK, and Akt phosphorylation, respectively. Typical immunoblots (upper panel) and the average ± SE (n = 2-4) (lower panel) are shown.

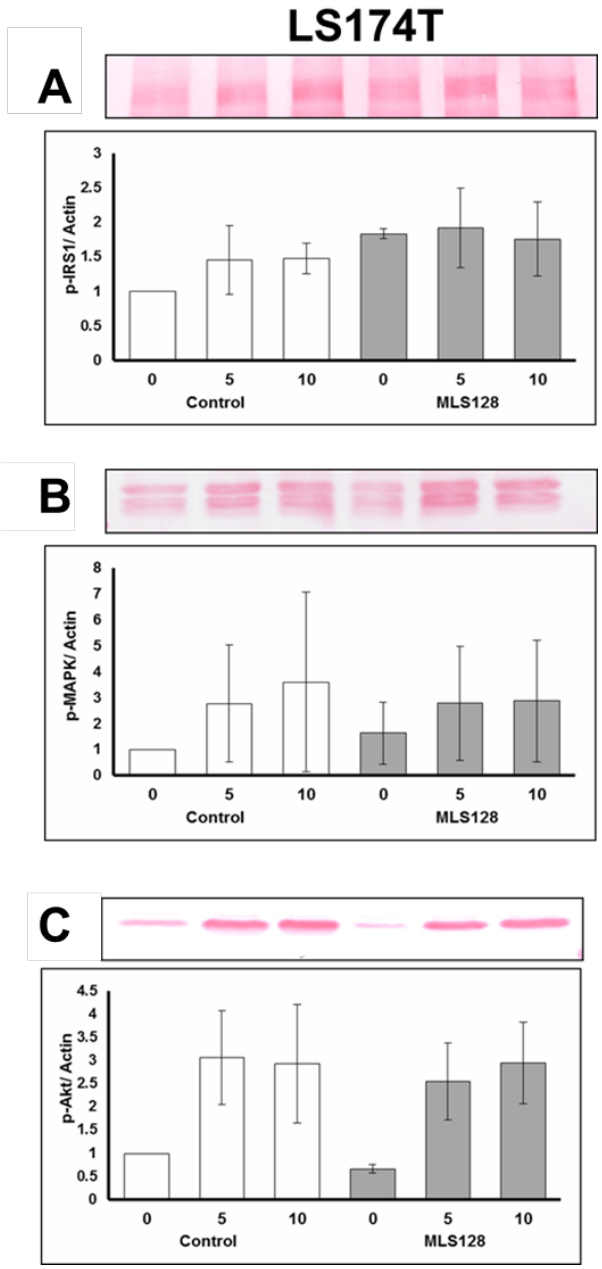

Figure 12. Effects of MLS128 on IGF-IR signaling in the LS174T colon cancer cell line. Briefly, 50 ng/mL of IGF-I was added to cells cultured in SFM containing 0.1% BSA (white bars) or 25 µg/mL of MLS128 (grey bars). After incubation for 5 or 10 min, cells were subjected to solubilization. The solubilized proteins (5 µg per lane) were separated by SDS-PAGE and subjected to Western blotting using primary antibodies against p-Tyr (A), p-MAPK (B), and p-Akt (C) for detection of IRS-1, MAPK, and Akt phosphorylation, respectively. Typical immunoblots (upper panel) and the average ± SE (n = 2-4) (lower panel) are shown.

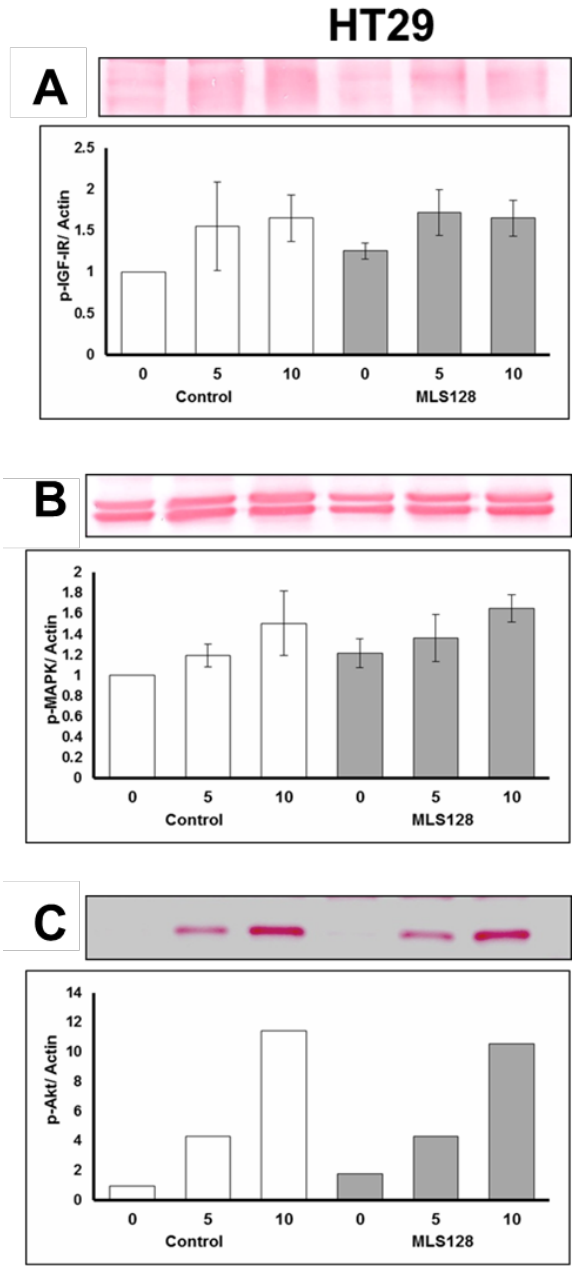

Figure 13. Effects of MLS128 on IGF-IR signaling in the HT29 colon cancer cell line. Briefly, 50 ng/mL of IGF-I was added to cells cultured in SFM containing 0.1% BSA (white bars) or 25 µg/mL of MLS128 (grey bars). After incubation for 5 or 10 min, cells were subjected to solubilization. The solubilized proteins (5 µg per lane) were separated by SDS-PAGE and subjected to Western blotting using primary antibodies against p-Tyr (A), p-MAPK (B), and p-Akt (C) for detection of IRS-1, MAPK, and Akt phosphorylation, respectively. Typical immunoblots (upper panel) and the average ± SE (n = 2-4) (lower panel) are shown.

2.5.4 Effects of 1H7 or MLS128 treatment on IGF-IR levels

Since a previous study suggested that MLS128 inhibits LS180 cell growth via down-regulation of IGF- IR, the amounts of IGF-IR in three colon cell lines after 1H7 or MLS128 treatment were determined by IB. After treatment with MLS128 or 1H7 for 1, 2, and 3 days, cells were solubilized. Cell lysates were immunoblotted with anti-IGF-IR β subunit antibody to ascertain whether or not down-regulation of the IGF-IR molecules occurred in the three colon cancer cell lines after each mAb treatment.

Down-regulation of IGF-IR by 1H7 was clearly evident in all three colon cancer cell lines (Fig. 14). Among the three cell lines, HT29 cells (Fig. 14C, black bars) had the most significant IGF-IR down-regulation by 1H7. These results are consistent with the hypothesis that 1H7- induced IGF-IR down-regulation plays a role - at least in part - in inhibiting the growth of colon cancer cells.

As shown in Fig. 14, MLS128 treatment of three colon cancer cell lines resulted in only slight down-regulation of IGF-IR in HT29 cells on Days 2 and 3 (Fig. 14C, grey bars), but the extent of this down-regulation paled in comparison to that induced by 1H7 (Fig. 14). MLS128 treatment of LS180 cells did not cause a reduction in IGF-IR as was previously reported. Thus, the results of the current study disagreed with those of a previous study indicating that MLS128 down-regulated IGF-IR in 180 cells.

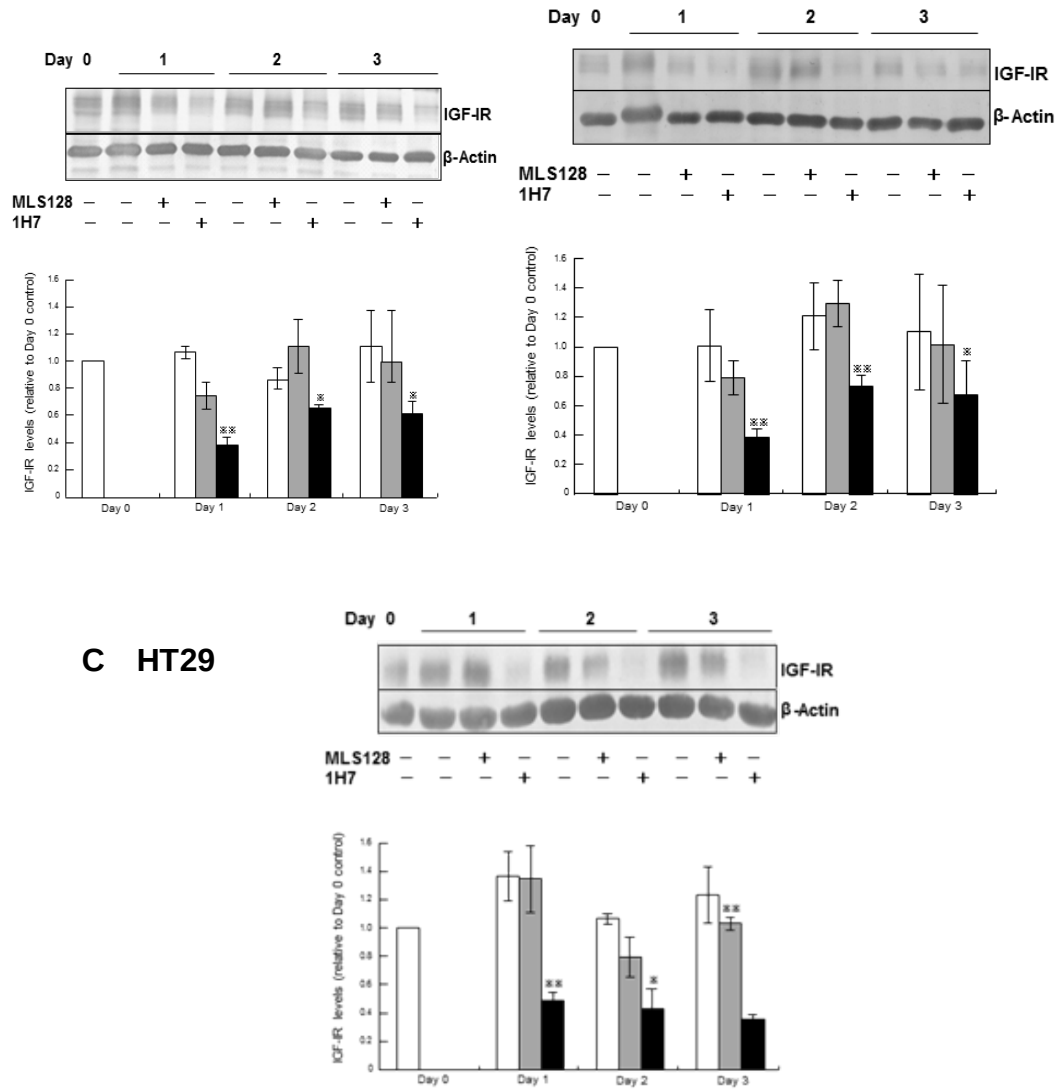

Figure 14. Effects of 1H7 or MLS128 treatment on cellular levels of IGF-IR. Briefly, colon cancer cells were cultured in respective media containing 1% FBS in the presence or absence of MLS128 (25 μg/mL) or 1H7 (0.36 μg/mL) for 24 (Day 1), 48 (Day 2), and 72 h (Day 3). Cell lysates (2 μg protein per lane) were subjected to Western blotting using primary antibodies, anti-IGF-IR β subunit, and anti-β-actin and then subjected to color development using biotin-labeled secondary antibodies and an alkaline phosphatase kit. The IGF-IR levels were normalized to β-actin levels. White bars represent controls, which are IGF-IR levels from cells untreated with mAb. The grey and black bars represent IGF-IR levels in cells treated with MLS128 and 1H7, respectively. The average values of these protein levels on Days 1, 2, and 3 were calculated with respect to Day 0. * $p < 0.05$; ** $p < 0.01$.

2.5.5 Effects of MLS128 treatment on 110 kDa GP levels

Figure 15 shows the MLS128 IB of cell lysates prepared from LS180, LS174T, and HT29 cells after treatment with MLS128 or 1H7 for 1, 2, and 3 days.

Although disappearance of the 110 kDa GP band was not as apparent as was seen in IGF-IR IB, partial disappearance of the 110 kDa GP was noted in all three colon cancer cell lines when they were treated for 3 days with MLS128. Of the three colon cancer cell lines examined, however, HT29 cells treated with MLS128 had the most significant reduction in 110 kDa GP, suggesting that MLS128 binding to 110 kDa GP is possibly involved in inhibiting HT29 cell growth.

In contrast, the 110 kDa GP in cells treated with 1H7 remained at the same levels as in non-treated control cells (Fig. 15), suggesting that 1H7 treatment did not affect 110 kDa GP levels.

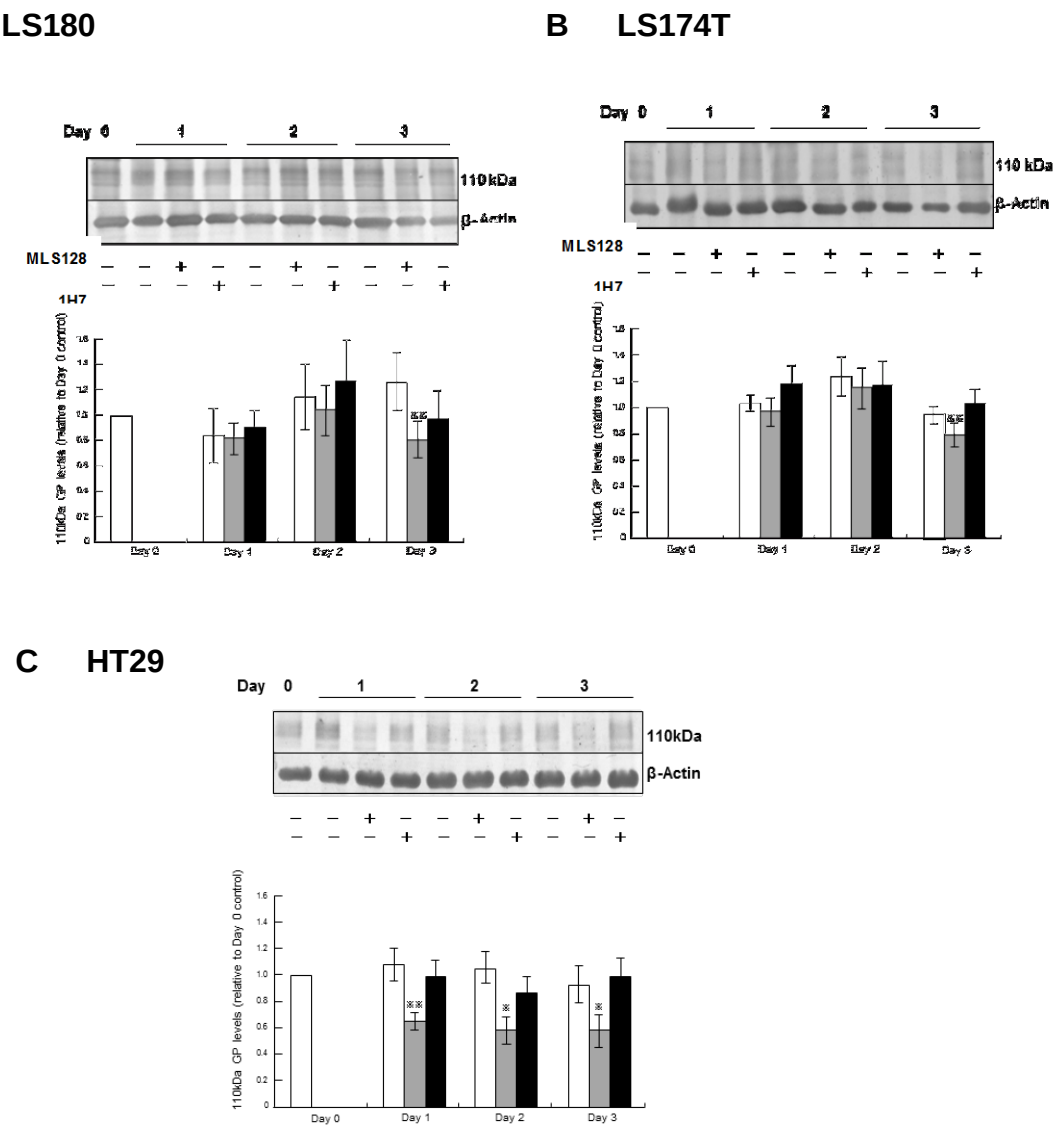

Figure 15. Effects of 1H7 or MLS128 treatment on cellular levels of 110 kDa GP. Briefly, colon cancer cells were cultured in respective media containing 1% FBS in the presence or absence of MLS128 (25 µg/mL) or 1H7 (0.36 µg/mL) for 24 (Day 1), 48 (Day 2), and 72 h (Day 3). Cell lysates (2 µg protein per lane) were subjected to Western blotting using primary antibody MLS128 and anti-β-actin and then subjected to color development using biotin-labeled secondary antibodies and the alkaline phosphatase kit. The 110 kDa levels were normalized to β-actin levels. White bars represent controls, which are 110 kDa levels from cells untreated with mAb. The grey and black bars represent 110 kDa levels in cells treated with MLS128 and 1H7, respectively. Average values of these protein levels on Days 1, 2, and 3 were calculated with respect to Day 0. * $p < 0.05$; ** $p < 0.01$.

2.5.6 Expression of growth-related molecules

Since previous studies suggested that the growth of colon cancer cells may be mediated by IGF-IR, EGFR, and c-Met (Morita *et al*., 2009, Zhang *et al*., 2008, Zeng *et al.,* 2004), expression of those proteins was measured in three colon cancer cell lines and control MCF-7 breast cancer cells. Western blot analyses were carried out using two concentrations of colon or breast cancer cell lysates. Typical results of Western blots with antibodies against six molecules are shown in Fig. 16.

Three colon cancer cell lines expressed the IGF-IR protein. LS174T and HT29 cells expressed the protein at a level similar to that found in MCF- 7 breast cancer cells but the level of expression in LS180 cells appeared to be lower than that in other cell lines (Fig. 16-1 A). When blotted with MLS128, all three colon cancer cell lines had similar levels of 110 kDa GP but 110 kDa GP was not detected in MCF- 7 cells, which instead expressed MLS128-detectable bands with higher molecular masses (Fig. 16-1 B). The MLS128 IB of cell lysates in this study confirmed previous results for MLS128 IB when cell membranes were prepared from LS180, HT29, and MCF-7 cells. All three colon cancer cell lines contained similar levels of EGFR and c-Met but MCF-7 breast cancer cells had almost no expression of EGFR and c-Met (Fig. 16-2 C and D). These results suggest that different signaling pathways are used to promote growth in colon and breast cancer cells.

In addition, IB experiments were carried out using anti-E-cadherin and CD44 antibodies since E-cadherin and CD44 are reported to have a size close to that of 110 kDa GP, which MLS128 binds to. Interestingly, LS180 cells did not express E-cadherin whereas two other colon cancer cell lines and the MCF-7 breast cancer cell line expressed similar levels of E-cadherin (Fig. 16-3 E). Although the three colon cancer cell lines had comparable patterns of anti-CD44 reactive bands corresponding to splice variants of > 80 kDa, LS180 cells appear to express higher levels of those molecules than LS174T and HT29 cells (Fig. 16-3 F). In contrast, MCF-7 breast cancer cells displayed almost no anti-CD44 reactive bands.

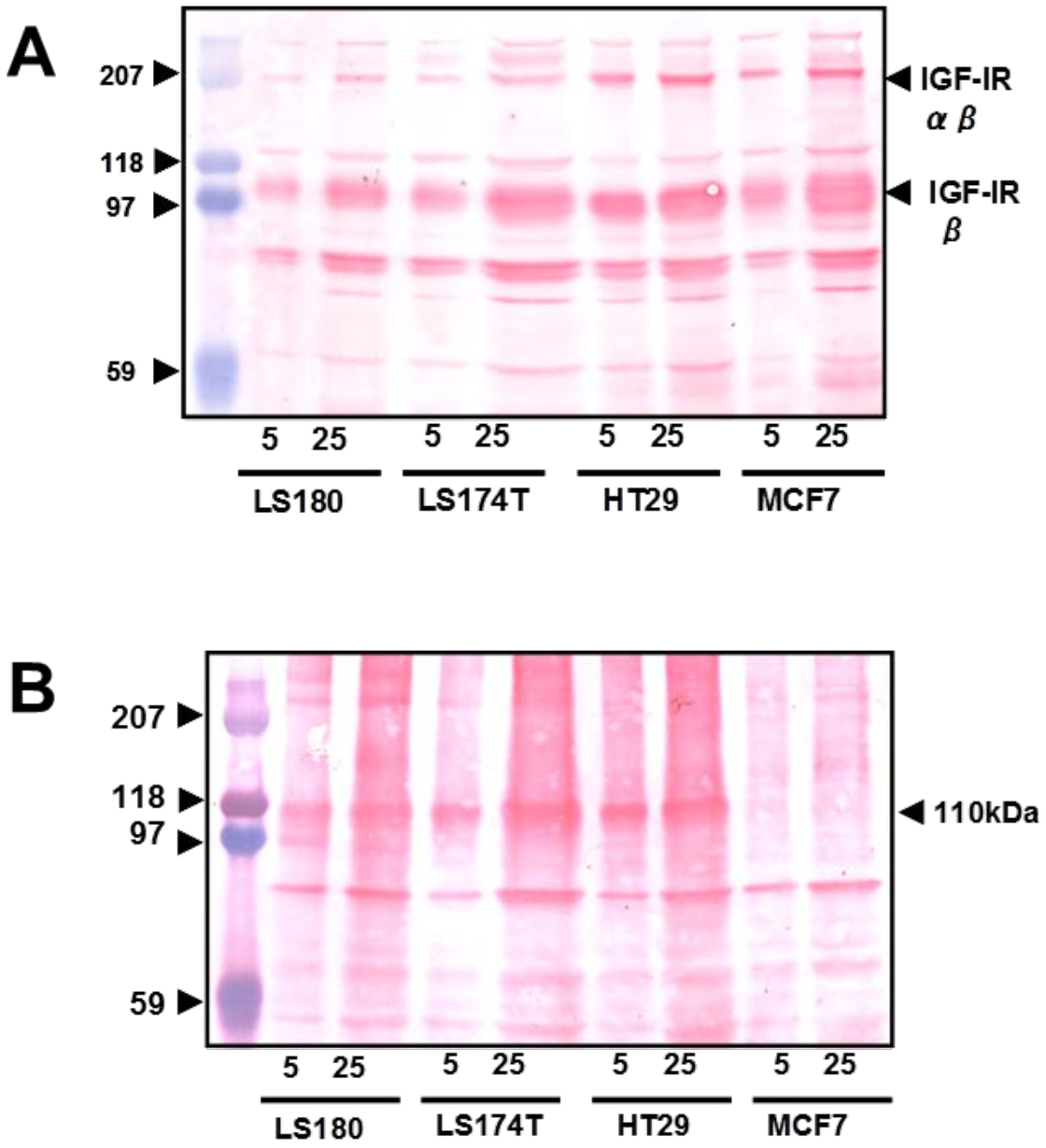

Figure 16-1. Different sets of growth-related molecules are expressed in colon and breast cancer cells. Expression of IGF-IR, MLS128 binding protein (110 kDa GP), and four other proteins was compared using Western blotting with 5 and 25 µg protein each of LS180, LS174T, HT29, and MCF7 cell lysates. The primary antibodies used were anti-IGF-IR (A) and MLS128 (B). Bound primary antibodies were detected using biotin-labeled secondary antibodies.

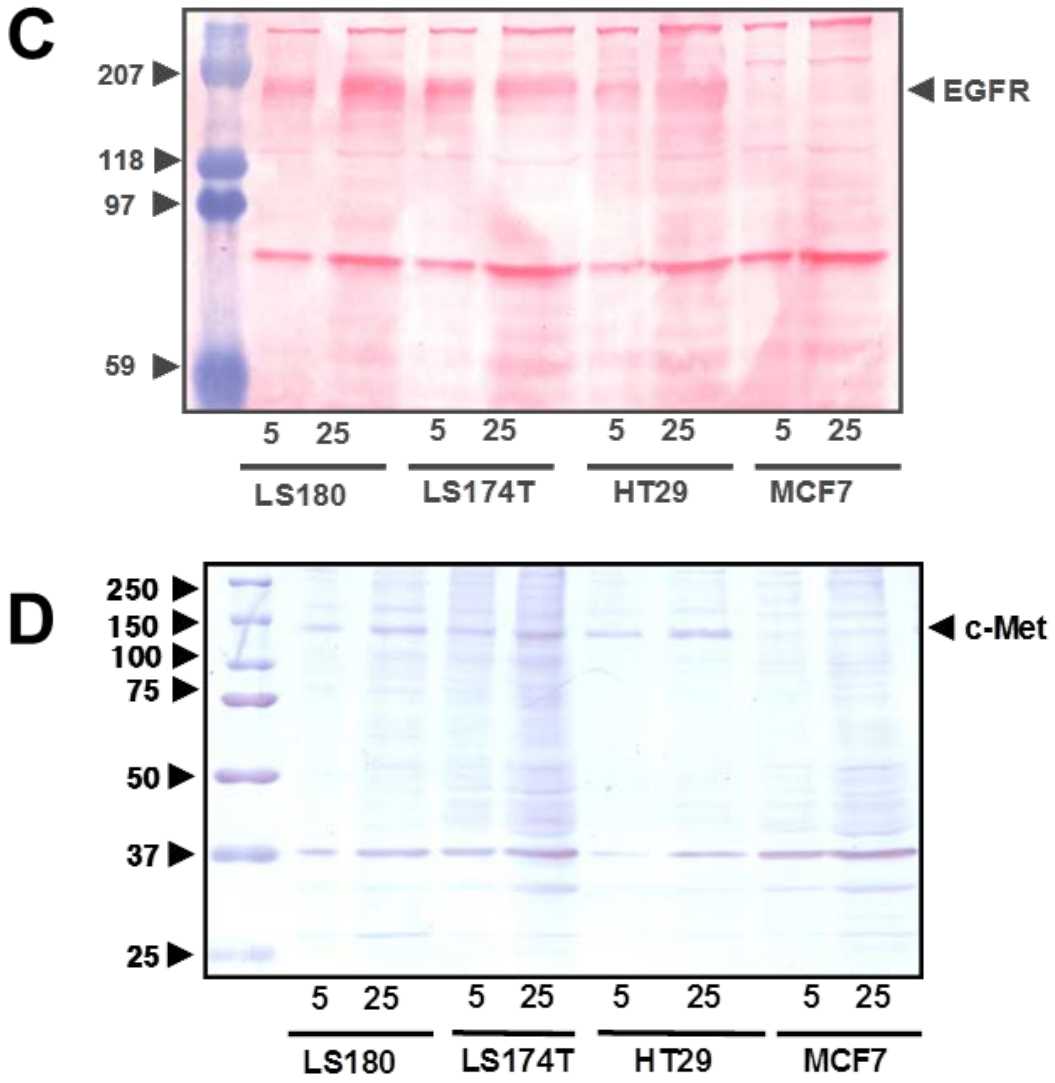

Figure 16-2. Different sets of growth-related molecules are expressed in colon and breast cancer cells. Expression of IGF-IR, MLS128 binding protein (110 kDa GP), and four other proteins was compared using Western blotting with 5 and 25 µg protein each of LS180, LS174T, HT29, and MCF7 cell lysates. The primary antibodies used were anti-EGFR (C) and anti-c-Met (D). Bound primary antibodies were detected using biotin-labeled secondary antibodies for C. Alternatively, bound primary antibodies were detected with HRP-conjugated secondary antibodies and color development using Ez West blue (D). In contrast to the relatively abundant proteins shown in C, the proteins shown in D were not readily detected with biotin-labeled secondary antibodies due to the existence of non-specific 125, 75, and 73 kDa proteins functioning as endogenous biotin-containing enzymes in cells. Thus, an alternative method was used to detect sparse proteins (D).

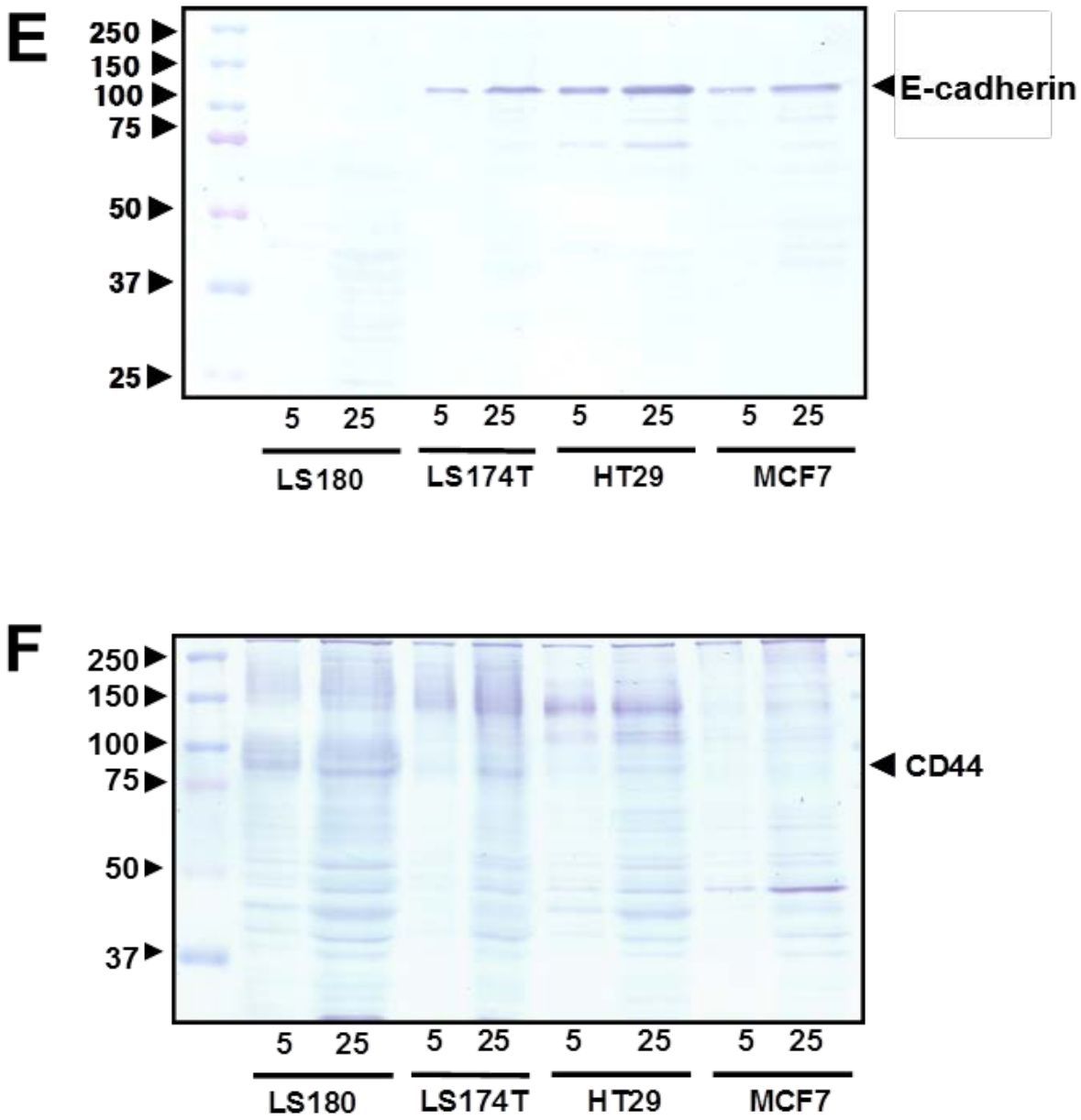

Figure 16-3. Different sets of growth-related molecules are expressed in colon and breast cancer cells. Expression of IGF-IR, MLS128 binding protein (110 kDa GP), and four other proteins was compared using Western blotting with 5 and 25 µg protein each of LS180, LS174T, HT29, and MCF7 cell lysates. The primary antibodies used were anti-E-cadherin (E), and anti-CD44 (F). Bound primary antibodies were detected with HRP-conjugated secondary antibodies and color development using Ez West blue.

The results of the IB experiments are summarized in Table 2, which clearly shows that (i) colon and breast cancer cells express vastly different sets of growth-related molecules, and

(ii) the three colon cancer cell lines have somewhat similar but nonetheless distinctive patterns of these molecules.

Table 2. Expression of growth-related cell surface molecules in LS180, LS174T, and HT29 colon cancer cells in comparison to MCF-7 breast cancer cells.

Levels of expression of IGF-IR, 110 kDa GP, EGFR, c-Met, E-cadherin, and CD44 are summarized from the results shown in Fig. 16.

	LS180	LS174T	HT29	MCF-7
IGF-IR	+	++	++	++
110 kDa GP	+	+	+	±
EGFR	+	+	+	±
c-Met	+	++	+	±
E-cadherin	-	+	++	+
CD44	++	+	+	±

2.6 Discussion

This study used three established colon cancer cell lines in an effort to reveal the potential roles of IGF-IR signalling in the growth of colon cancer cells and its possible interaction with MLS128-induced inhibition of cell growth.

The three colon cancer cell lines expressed IGF-IR. Treatment of cells with 1H7 caused inhibition of their growth and down-regulation of IGF-IR. 1H7 inhibited cell growth by 30-40%, indicating that 60-70% of cell growth must be mediated by signalling pathways other than IGF-IR signalling. MLS128 did not affect the phosphorylation of downstream signalling molecules stimulated by IGF-I, such as IRS-1, MAPK, and Akt. These results suggest that MLS128-induced inhibition of the growth of colon cancer cells is independent of IGF-IR signalling.

Colorectal cancer is the world's third most common cancer, and further studies are needed to determine the mechanisms by which its growth is inhibited. This study did not extensively examine levels of expression of growth-related molecules in colon cancers, but Fig. 16 provides insight into growth signalling in each colon cancer cell line.

Transcriptomes and/or proteomics could be used to examine other molecules and develop a profile of each colon cancer cell line. Such work could eventually provide a model for development of cancer therapeutics. As far as *in vivo* studies are concerned, a very recent genome-scale analysis of 276 human colon and rectal cancer samples found amplification of IGF-II in addition to the expected mutations (Cancer Genome Atlas Network, 2012). This new finding is consistent with the results of the present study, which found that growth of colon cancer cells is IGF-dependent but only to a degree.

Western blot analyses were carried out in an effort to narrow down other growth signalling pathways that MLS128 may interact with (Fig. 16). EGFR was expressed in all colon cancer cell lines, indicating that their growth is likely to be mediated by this receptor as well. LS180 cell growth was found to be EGF-dependent (Zamri *et al.* unpublished findings). c-Met signalling is reportedly involved in the growth of HT29 cells. c-Met expression in colon and breast cancer cells was determined using Western blotting, and the three colon cancer cell lines expressed c-Met. These results suggest that growth of colon cancer cell lines is likely to be mediated by IGF-I, EGF, and HGF, the ligand for

c-Met. Unlike colon cancer cells, MCF-7 breast cancer cells did not express either EGFR or c-Met.

The results described here are thus significant in that two colon cancer cell lines may use growth signalling similar to that in HT29 cells, which most signalling studies have thus far reported. However, their role in the growth of each cell line has to be carefully investigated since only three cell lines were compared but subtle differences were clearly noted. In fact, preliminary data indicate that the growth of LS180 cells was not stimulated by HGF (Oura *et al.,* unpublished findings). More studies with established cell lines would shed light on the mechanisms of the growth of colon cancer cells and could eventually lead to the design and development of cancer therapeutics.

This study revealed one significant aspect of the nature of colon cancer cells. Namely, MLS128 binding to the 110 kDa GP on colon cancer cell lines apparently resulted in inhibition of growth whereas MCF-7 cells expressed GPs with higher molecular masses as MLS128 binding proteins. In a previous study, those differences were revealed by Western blotting using membrane fractions. The current study used cell lysates for Western blotting and noted the same differences, thus suggesting that quantitative analyses of receptors and other signal molecules can be easily carried out using cell lysates instead of cell membranes. Given this, two sets of experiments were conducted as shown in Figs. 14 and 15. Figure 14 shows that anti- IGF-IR antibody caused down-regulation, or more accurately speaking, degradation of the receptors in three colon cancer cell lines. In contrast, MLS128 did not down-regulate IGF-IR in colon cancer cell lines. This result rules out the original hypothesis that the down-regulation of IGF-IR is one possible mechanism by which MLS128 inhibits LS180 cell growth.

Treating three colon cancer cell lines with MLS128 for 3 days resulted in inhibition of their growth and obvious disappearance of the 110 kDa band as indicated by IB with MLS128. The disappearance of the110 kDa band was clearly evident in HT29 cells on Days 1, 2, and 3 after the mAb treatment but the disappearance of the 110 kDa band was seen only on Day 3 after the treatment of LS180 and LS174T cells. The disappearance of the 110 kDa band could be explained by either the loss of the Tn-antigen epitopes on the protein backbone or degradation of the protein backbone itself. Antibodies recognizing the protein

backbone of 110 kDa GP are needed to identify whether protein degradation has occurred or Tn-antigen epitopes have been lost once colon cancer cells have been treated with MLS128. Identification of the 110 kDa GP is the next important step in producing antibodies against the 110 kDa GP and understanding MLS128's inhibition of cell growth.

In conclusion, the present study confirms previous findings and facilitates additional understanding of cell growth and IGF-IR. By binding to IGF-IR, 1H7 inhibited the growth of all three colon cancer cell lines studied. This inhibitory action was more significant than that of MLS128. In addition, growth of all three colon cancer cell lines was found to be IGF-I dependent (Fig. 10). Furthermore, IGF-I activated downstream signaling via Akt and MAPK phosphorylation. Contrary to the initial hypothesis, however, MLS128 did not significantly affect IGF-IR signaling. IGF-IR was significantly down-regulated by 1H7 in all three colon cancer cell lines, and especially in HT29 cells. However, 1H7 treatment did not affect 110 kDa GP levels. In contrast, MLS128 treatment caused partial disappearance of 110 kDa GP in all three cancer cell lines and this effect was most significant in HT29 cells. However, MLS128 did not appear to affect IGF-IR levels except in HT29 cells cultured for 3 days (Fig. 14 and 15)

Considerably more work using HT29 cells will need to be done to determine the association between IGF-IR and 110 kDa GP and other signaling molecules that may be involved in the inhibitory action of MLS128. The nature of MLS128 binding protein 110 kDa GP and its identity may also be a vital clue to answer many of the questions regarding signaling pathway cascades activated by MLS128.

Chapter 3

Characterization of anti-Tn-antigen MLS128 binding proteins involved in inhibiting the growth of human colorectal cancer cells

3.1 Summary

This chapter investigated the nature of a 110 kDa GP (MLS128 cell surface-binding protein) and its possible association with IGF-IR.

SDS-PAGE and immunoblotting (IB) confirmed that MLS128 treatment for 3 days caused down-regulation of IGF-IR and disappearance of 110 kDa GP in HT29 colon cancer cells. Immunoprecipitation/IB experiments, however, failed to provide evidence of a direct association between the two molecules in HT29 cells. In LS180 and HT29 colon cancer cells, both 110 kDa GP and IGF-IR were found in microdomains.
Treatment of these cells with MLS128 for 3 days caused a reduction in the IGF-IR and 110 kDa GP associated with microdomains.

Two-dimensional PAGE-IB of LS180 and HT29 cell lysates revealed MLS128-stainable spots at similar positions, suggesting several candidate proteins.

Although the 110 kDa GP has been identified as the receptor for MLS128, which is involved in inhibiting the growth of colon cancer cells, its origin must be investigated further.

3.2. Introduction

A previous study (Morita *et al*., 2009) reported that MLS128 significantly inhibits breast and colon cancer cell growth and suggested involvement of IGF-I receptor signaling in MLS128's inhibition of the growth of LS180 colon cancer cells.

As stated in the previous chapter, MLS128 bound specifically to 110 kDa GP in the three colon cancer cell lines studied and IGF-IR signaling was not associated with MLS128's inhibition of the growth of LS180 and LS174T cells. MLS128 treatment did not significantly result in IGF-IR down-regulation as was expected. However, MLS128 appeared to affect HT29 more than LS180 and LS174T cells. The possibility of a link between IGF-IR- and 110 kDa GP-mediated growth signaling pathways in HT29 cells still needs to be determined.

Thus, this chapter discusses the characterization of the 110 kDa GP in order to understand MLS128's inhibitory action on cell growth in HT29 and LS180 colon cancer cells. Specifically, the original working hypothesis regarding the interaction between IGF-IR and the 110 kDa GP has been intensively tested using HT29 colon cancer cells.

3.3 Materials

Production and characterization of MLS128 were as previously described in Chapter 1.

LS180 and HT29 human colon adenocarcinoma cells were obtained from the American Tissue Type Culture Collection.

Rabbit anti-IGFIRβ was purchased from Cell Signaling Technology (Beverly, MA, USA).

Rabbit anti-SFK (SRC 2; sc-18) was purchased from Santa Cruz Biotechnology (Santa Cruz, CA, USA).

Anti-rabbit or -mouse secondary antibody labeled with biotin was from Kirkegaard & Perry Laboratories (Gaithersburg, MD, USA).

Cell culture media (DMEM and McCoy's 5A) were purchased from Invitrogen (Carlsbad, CA).

3.4 Methods

Cell culture

LS180 cells were cultured in DMEM containing 10% fetal bovine serum (FBS) supplemented with 4.5 mg/mL D-glucose and 110 μg/mL pyruvic acid. HT29 cells were cultured in McCoy's 5A containing 10% FBS. All culture media included a 1% penicillin-streptomycin solution (Sigma-Aldrich).

Effects of 1H7 or MLS128 on the growth of colon cancer cells

Cells (1 x 10^4) were plated in wells of a 96-well plate and cultured in 100 μL of respective media containing 10％FBS for 24 h. Attached cells were then washed twice with 10 mM phosphate buffer, pH 7.4, containing 0.14 M NaCl (PBS), and cultured in 100 μL of media containing 1% FBS in the presence or absence of MLS128 (25 μg/mL) or 1H7 (0.36 μg/mL). After culturing for 72 h, cell growth was determined using a CCK-8 cell counting kit (Dojindo, Kumamoto, Japan) in accordance with the manufacturer's instructions. Absorbance at 450 nm was measured with a plate reader (Bio-Rad, Hercules, CA, USA). Quadruple wells were prepared for each data point.

Western blotting

HT29 colon cancer cells were collected by scraping. They were then centrifuged at 200 × g for 5 min and solubilized in 50 mM Tris-HCl buffer, pH 7.4, containing 1% NP40, 2 mM EDTA, 100 mM NaCl, 10 mM sodium orthovanadate, 1 mM PMSF, and protease inhibitors (Sigma-Aldrich P2714) (Lysis buffer A) on ice for 15 min. Supernatants were obtained from solubilized cells by centrifugation at 17,000 × g for 10 min. Protein concentrations were measured using the Bradford method. The solubilized proteins (2 μg) were separated by sodium dodecyl sulfate-polyacrylamide gel electrophoresis (SDS-PAGE) and transferred to polyvinylidene difluoride (PVDF) membranes. The membrane was blocked with 3% BSA in 50 mM Tris-HCl buffer, pH 7.4, containing 0.15 M NaCl and 1% Tween 20 (TBST) for 1 h at room temperature. Western blotting was carried out with anti-IGF-IR and MLS128 as primary antibodies. Bound primary antibodies

were then detected with biotin-labeled secondary antibodies using a Vectastain ABC-Amp kit and an alkaline phosphatase kit (Vector Laboratories, Inc. Burlingame, CA, USA).

Effects of 1H7 or MLS128 treatment on IGF-IR and 110 kDa GP levels in HT29 colon cancer cells

HT29 colon cancer cells (8×10^5) were cultured in media containing 10% FBS for 24 h in wells of 6-well plates. Cells were then cultured in the media containing 1% FBS in the presence or absence of MLS128 (25 μg/m L) or 1H7 (0.36 μg/mL). After culturing for 24, 48 and 72 h, cells were collected and solubilized in 50 μL of the lysis buffer as described above. The solubilized proteins (2 μg per lane) were separated by SDS-PAGE and transferred to PVDF membranes. Western blotting was performed thereafter as described above using primary antibodies against 110 kDa GP (MLS128), IGF-IR β subunit, and β-actin. Bound primary antibodies were visualized and then analyzed using an NIH Image 1.63 Analysis system (Research Services Branch, the National Institute of Mental Health, USA).

Immunoprecipitation (IP) and immunoblotting (IB) of IGF-IR or 110 kDa GP using 1H7, MLS128, and control antibodies from HT29 cell lysates

Whether IGF-IR and 110 kDa are associated or not was determined by IP with anti-IGF-IR, MLS128, or control IgG_3 from cell lysates followed by IB. HT29 colon cancer cells cultured in media containing 10% FBS were collected from 15-cm dishes by scraping and then centrifuged at 200 × g for 5 min. After they were washed with PBS, the cells were suspended in 1 mL of the lysis buffer on ice for 15 min. Supernatants obtained by centrifugation at 17,000 × g for 15 min. were incubated with 20 μL of protein G Sepharose at 4ºC for 1 h with rotation. After centrifugation at 17,000 × g for 10 min, protein concentrations of the supernatants were determined. Lysis buffer A was added to yield a concentration of 500 μg protein/200 μL, to which 10 μg of anti-IGF-IR, MLS128, or IgG_3 was mixed by rotation at 4ºC overnight. To bring down associated protein complexes, 25 μL of 50% protein G Sepharose was added to each tube and the tubes were

rotated for 30 min. The gels were recovered by centrifugation at 17,000 × g for 10 min and then suspended in 1 mL of TBS-0.05% Tween (TBST). After this washing process was repeated 5 times, the gels were suspended in 30 µL of 1xSDS-PAGE sample buffer and then heated at 100ºC for 5 min. IP samples were analyzed by Western blotting using anti-IGF-IR, MLS128, or anti-IgG_3 as described above.

Sucrose gradient fractionation of HT29 and LS180 cell lysates

All steps were carried out at 4°C as previously described (Kabayama *et al.,* 2005, Oneyama *et al*., 2009). HT29 and LS180 cells grown in 3 - 5 150-mm dishes were washed with chilled PBS and lysed in 2 mL lysis buffer (50 mM Tris–HCl, pH 7.4, 100 mM NaCl), containing protease inhibitors and 1 mM PMSF, 10 mM sodium vanadate, and 0.1 % NP40 on ice for 20 min. After centrifugation for 5 min at 1300 × g, supernatants (2 mL) were diluted with 2 mL of 85% (w/v) sucrose in 10 mM Tris-HCl, pH 7.5, containing 150 mM NaCl and 5 mM EDTA (TNE buffer). The diluted lysates were overlaid with 4 mL of 30% sucrose (w/v) and then with 4 mL of 5% sucrose (w/v) in TNE buffer in an ultracentrifuge tube. The samples were centrifuged at 39,000 rpm for 18 h in an SW41 rotor (Beckman Instruments, Palo Alto, CA), and fractions were collected from the top for IB analysis. Fractions were immunoblotted with anti-Src family kinase (SFK), which served as an internal marker for microdomains.

Two-dimensional gel electrophoresis

HT29 and LS180 cells (2×10^7) were lysed with 200 µL of 7 M urea, 2 M thiourea, 2% 3[(3-cholamidopropyl)dimethylammonio]-1-propanesulfonate (CHAPS), 2% sulfobetaine 10, 1% protease inhibitor cocktail (Sigma-Aldrich, St Louis, MO), and 65 mM dithiothreitol (DTT); 40 µL of the lysate was then subjected to two-dimensional gel electrophoresis. Two-dimensional gel electrophoresis was performed according to previously described methods. Briefly, isoelectric focusing was carried out on Immobiline DryStrips (pH 4-7, 18 cm; GE Healthcare, Buckinghamshire, UK) using a CoolPhoreStar IPG-IEF type-P apparatus (Anatech, Tokyo, Japan) for 18 h. The strips were equilibrated in 50 mM Tris-HCl,

pH 6.8, containing 6 M urea, 2% SDS, 30% glycerol, and 2% DTT and then electrophoresed on 10% polyacrylamide gels according to Laemmli's method. Proteins were visualized with Coomassie brilliant blue (CBB) and silver staining. For immunostaining, two-dimensional gels were transferred to an Immobilon-P Membrane (Millipore, Bedford, MA) and the membrane was stained with 0.4 μg/mL of MLS128 antibody followed by alkaline phosphatase-conjugated anti-mouse IgG (Zymed Laboratories, San Francisco, CA). Binding of MLS128 was visualized via a chromogenic method using 5-bromo-4-chloro-3-indolylphosphate (BCIP)/nitro blue tetrazolium (NBT) color development substrate (Promega, Fitchburg, WI) according to the manufacturer's instructions. Immunoprecipitates from HT29 and LS180 cell lysates by MLS128 were also separated on two-dimensional gels and immunoblotted under the same conditions described above.

Statistical analyses

Levels of cell growth and protein bands in Western blotting were expressed as means±SE from 3 or more experiments. An unpaired Student's t-test was used to compare the growth or intensity of the bands in two groups of experiments performed in the absence and presence of MLS128.

3.5 Results

3.5.1 Inhibition of HT29 growth by 1H7 or MLS128

1H7 or MLS128 treatment of three colon cancer cell lines - LS180, LS174T, and HT29 - for three days was previously found to significantly inhibit cell growth. Although the original hypothesis regarding a possible interaction between IGF-IR and 110 kDa GP-mediated signaling in LS180 cells was not substantiated, a possible link between IGF-IR and 110 kDa GP signaling in HT29 cells has not been excluded. As a first step to test this hypothesis, the time-course effects of 1H7 or MLS128 mAb treatment on cell growth were measured on Days 1, 2, and 3 (Fig. 17). 1H7 significantly inhibited cell growth from Day 1 to Day 3. While HT29 cell growth was inhibited by MLS128 on Days 1, 2, and 3, this inhibition was only significant on Day 3. These results confirm that both mAb treatments inhibit cell growth for 3 days, as was previously stated in Chapter 2, and they also indicate that 1H7 treatment has a more substantial effect than MLS128 treatment.

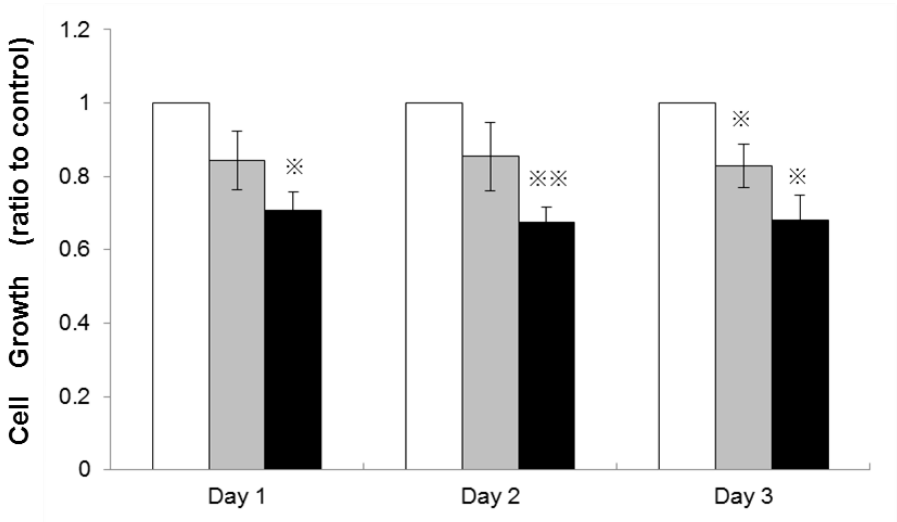

Figure 17. Effects of anti-IGF-IR 1H7 or anti-Tn-antigen MLS128 mAb on the growth of HT29 colon cancer cells. HT29 cells were cultured in the absence (control white bars) or presence of 1H7 (black bars) or MLS128 (grey bars) as described in the Methods. Cell proliferation was measured on Days 1, 2, and 3 using a CCK-8 cell counting kit (Dojindo, Kumamoto, Japan). Cell growth in the presence of either mAb on Days 1 to 3 was compared to the control (without Ab treatment): average ± SD (n=5). * $p < 0.05$; ** $p < 0.01$.

3.5.2 Effects of mAb treatment on IGF-IR or 110 kDa GP in HT29 cells

The receptors for 1H7 and MLS128 on HT29 cells were visualized using Western blotting with anti-IGF-IRβ (Fig. 18 A) and MLS128 (Fig. 18 B). The bands seen below the 94 kDa marker protein are 75 and 73 kDa endogenous biotin-containing enzymes (Robinson *et al.,* 1983), which served as an internal control. There were comparable levels of IGF-IR and 110 kDa GP expression in HT29 cells.

Treatment of HT29 cells with 1H7 resulted in the down-regulation of IGF-IR on Days 1-3 (Fig. 19 A, black bars). The levels of 110kDa GP decreased significantly in HT29 cells treated with MLS128 for 1-3 days (Fig. 19 B, grey bars). These results are consistent with those previously described in Chapter 2 for three colon cancer cell lines. MLS128 treatment caused down-regulation of IGF-IR on Days 2 and 3 (Fig. 19 A, grey bars). The effects were statistically significant on Day 3 but were not significant on Day 2. This result confirms the previous finding of down-regulation of IGF-IR in LS180 cells after MLS128 treatment to some extent and provided the impetus for the following experiments.

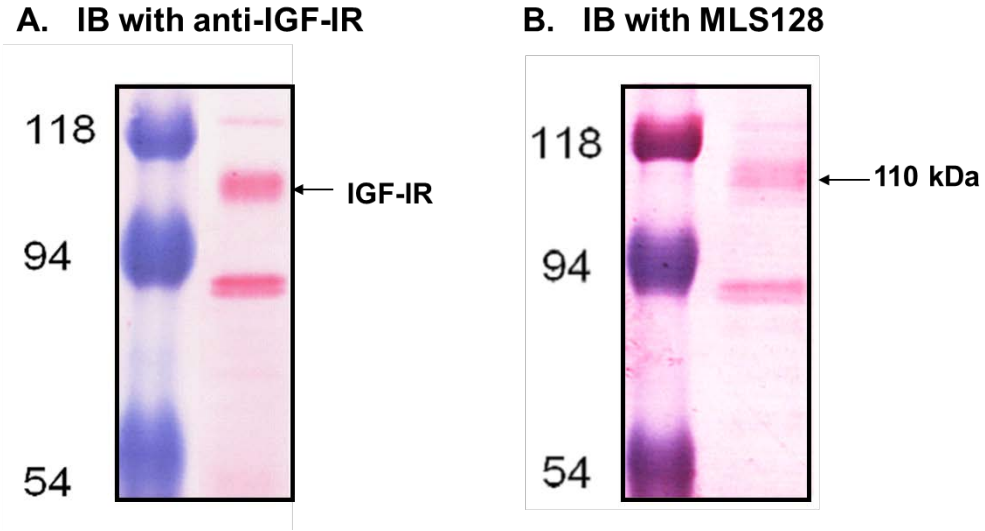

Figure 18. Expression of IGF-IR and 110 kDa GP in HT29 cells.
Solubilized proteins prepared from HT29 cells were separated by SDS-PAGE and immunoblotted with anti-IGF-IRβ (A) or MLS128 (B). The 75 and 73 kDa proteins stained are endogenous biotin-containing enzymes.

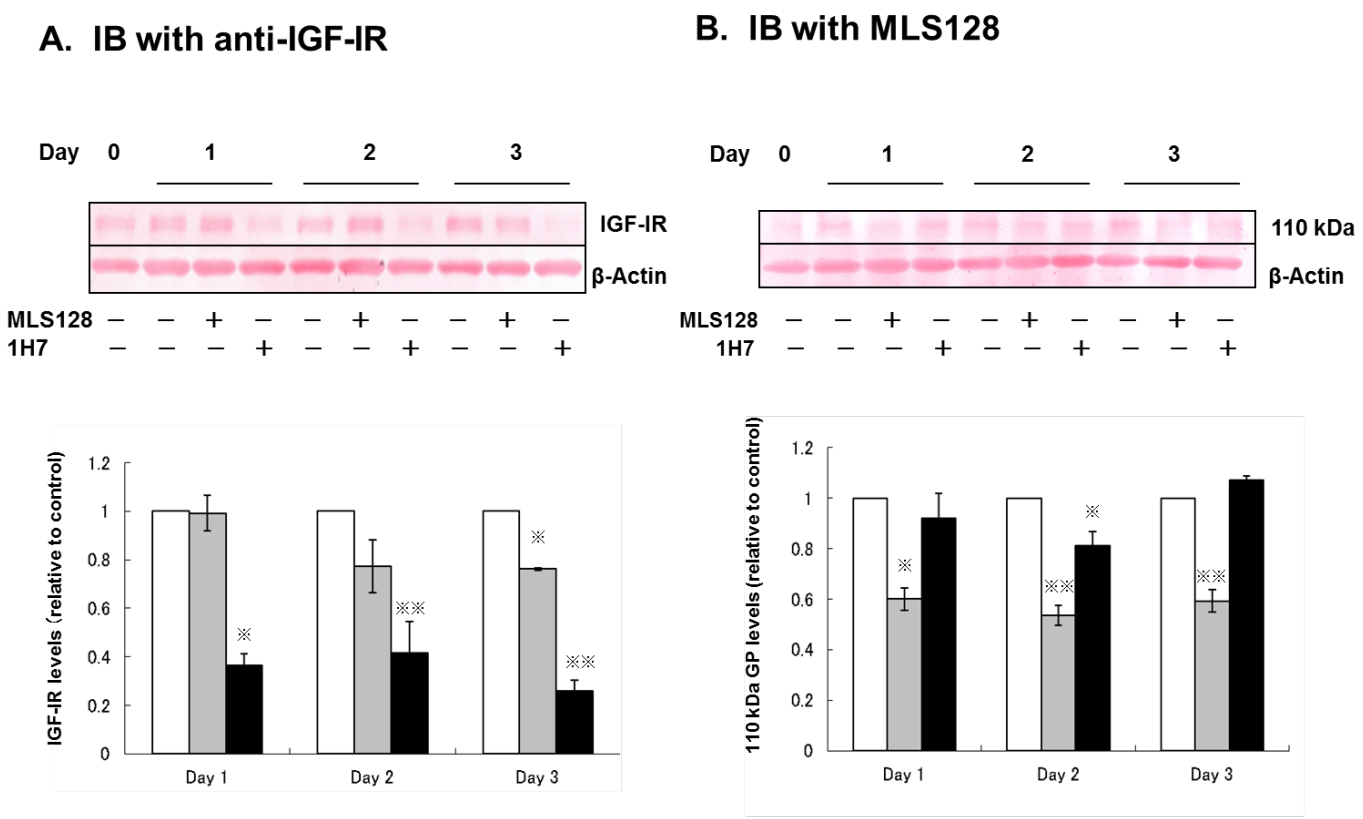

Figure 19. Expression of IGF-IR and 110 kDa GP (the receptor for MLS128) in HT29 cells.

Solubilized proteins (2 μg) prepared from HT29 cells were separated by SDS-PAGE and immunoblotted with anti-IGF-IRβ **(A)** or MLS128 **(B)** as described in the Methods. In the figures, the changes in the IGF-IR **(A)** and 110 kDa GP **(B)** band intensities are shown relative to the control on each day using the same sets of data for Fig. 14C and 15C, respectively, in which the band intensities on Days 1-3 were calculated with respect to the control on Day 0.

3.5.3 Association between IGF-IR and 110 kDa GP

To test whether IGF-IR and 110 kDa GP are associated in HT29 cells, IP/IB experiments were carried out using combinations of anti-IGF-IR, MLS128, and control IgG_3.

Since one of two independent experiments originally performed indicated possible co-immunoprecipitation of the two molecules, IP/IB was performed using 4 times the quantity of HT29 cell lysates used in previous experiments. In Fig. 20 A, IGF-IR (lane 1) was visible as expected. A band was seen at the IGF-IR position in MLS128-IP (lane 2), but a band was also seen in the control-IP (lane 3), suggesting that it must be non-specific. In anti-IGF-IR IP (Fig. 20 B lane 1), no band corresponding to 110 kDa GP (lane 2) was detected.

These results thus suggested no direct association between IGF-IR and 110kDa GP.

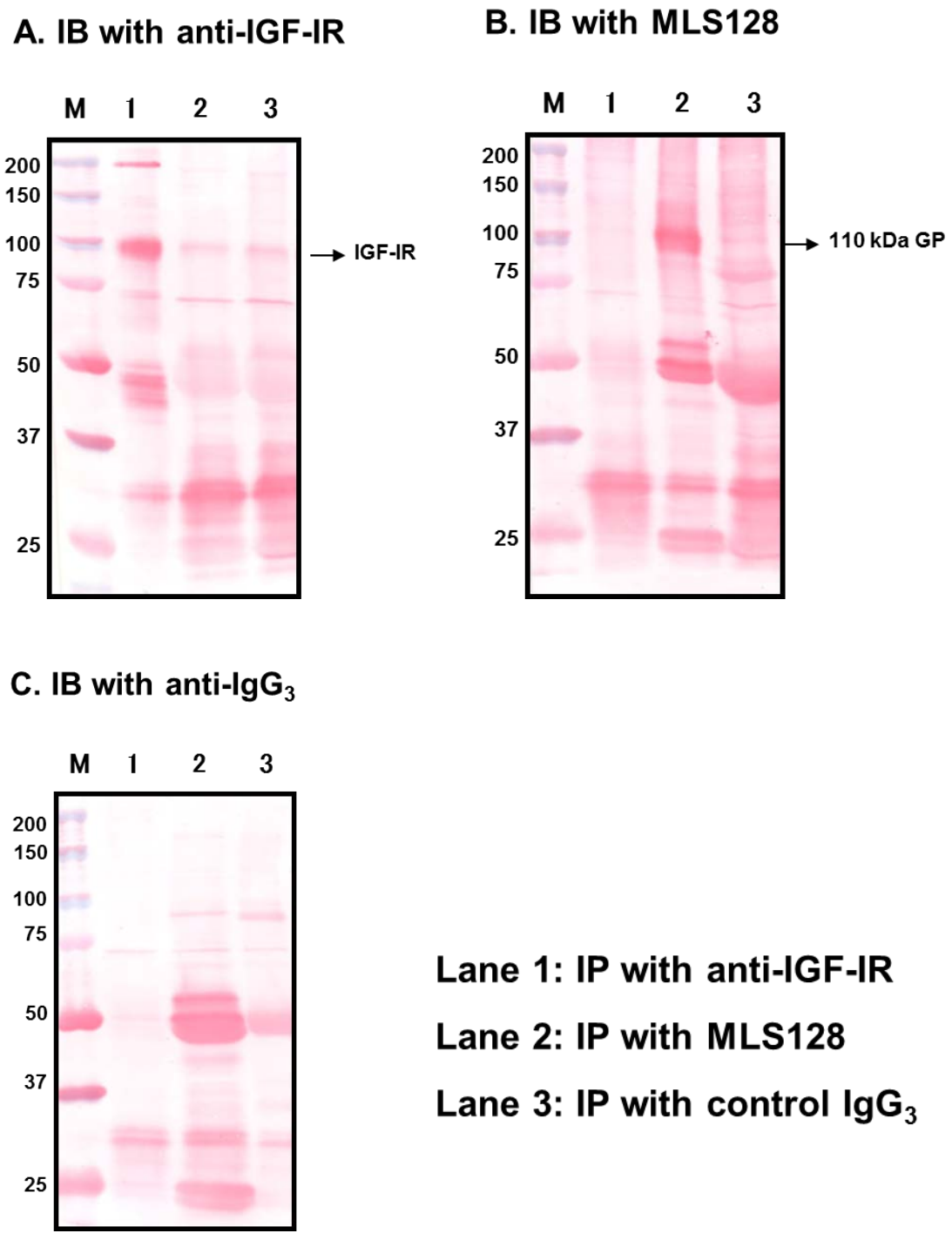

Figure 20. IP and IB of IGF-IR or 110 kDa GP using 1H7, MLS128, and control antibodies from HT29 cell lysates.

IP of HT29 cell lysates with anti-IGF-IR (1), MLS128 (2), or control IgG_3 (3) and IB with anti-IGF-IR **(A)**, MLS128 **(B)**, or anti-IgG_3 **(C)**.

3.5.4 Characterization of IGF-IR and 110 kDa GP in microdomains

Although there does not appear to be a direct association between IGF-IR and 110 kDa GP in HT29 cells, both molecules may exist in close proximity, such as in microdomains where receptors for various signaling are apparently located (Okamoto et al. 1998, Kabayama et al. 2005, Oneyama et al. 2009). Sucrose gradient fractionation of HT29 and LS180 cell lysates was performed to determine whether or not IGF-IR and 110 kDa GP exist in microdomains, and if so, to determine whether or not the treatment of cells with MLS128 for 3 days will affect the distribution of 110 kDa GP and/or IGF-IR.

In HT29 cells, both IGF-IR and 110 kDa GP were located in microdomains as shown in Fig. 21A and B, respectively. The same results were obtained with LS180 cells (Fig. 22B -MLS128). Anti-SFK blots indicated that the fractions 4-6 represent microdomains (Fig. 21 C, Fig. 22 SFK**)**

The distribution of IGF-IR and 110 kDa GP in HT29 and LS180 colon cancer cells was measured after MLS128 treatment to see if that distribution had changed. The results shown in Fig. 22 A (-MLS128) are, in fact, immunoblots derived from sucrose gradient centrifugation fractions of HT29 cells shown in Fig. 21 A, B, and C. Sucrose gradient fractionation experiments were actually performed in parallel, one for HT29 cells without MLS128 treatment (-MLS128) and the other for HT29 cells treated with MLS128 for 3 days (+MLS128), the results of which are summarized in Fig. 22 A. The same sets of data for LS180 cells are shown in Fig. 22 B.

In both HT29 and LS180 cells, treatment with MLS128 for 3 days was followed by a reduction in band intensities of IGF-IR, 110 kDa GP, and control SFK in microdomains (Fig. 22), suggested that the MLS128 treatment may have modulated microdomain organization.

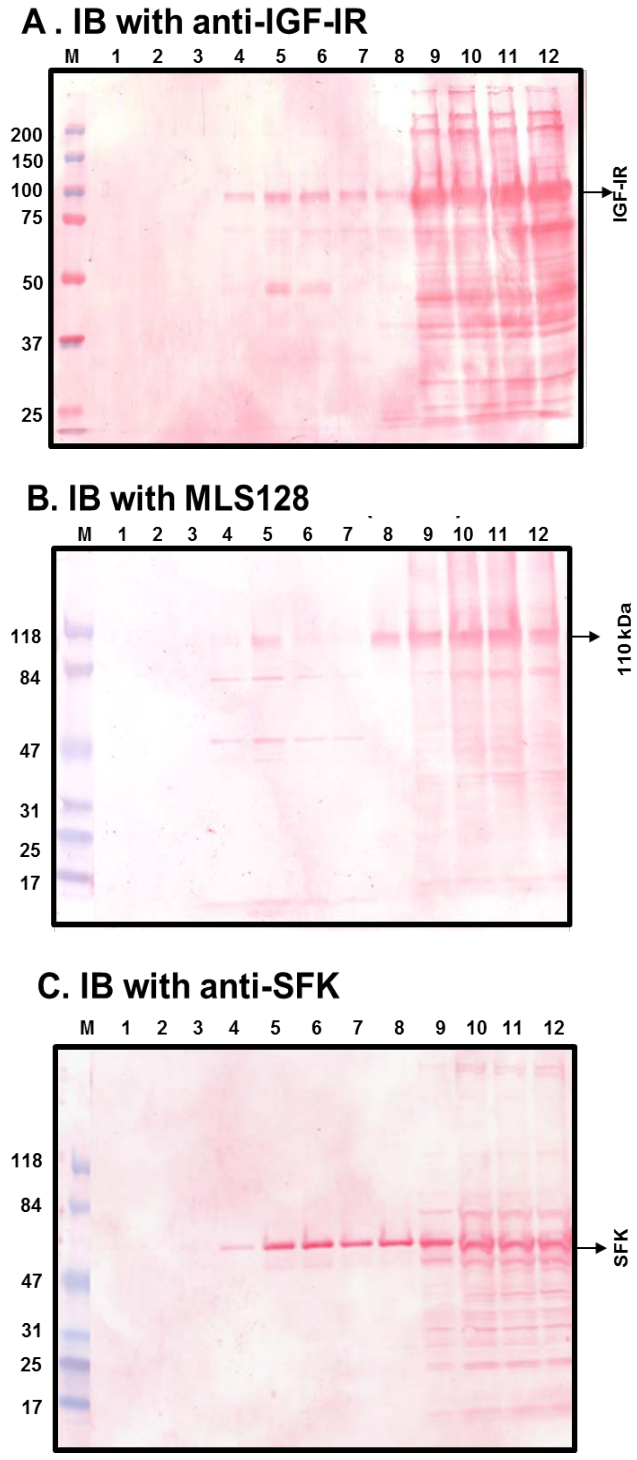

Figure 21. Characterization of HT29 cells by sucrose gradient fractionation. HT29 cell lysates were fractionated by sucrose gradient centrifugation and then fractions were immunoblotted as described in the Methods. **A.** IB of fractions 1-12 stored at –80 ºC for 3 years with anti-IGF-IR. **B.** IB of fresh fractions 1-12 with MLS128. **C.** IB of fresh fractions 1-12 with anti-SFK.

A HT29

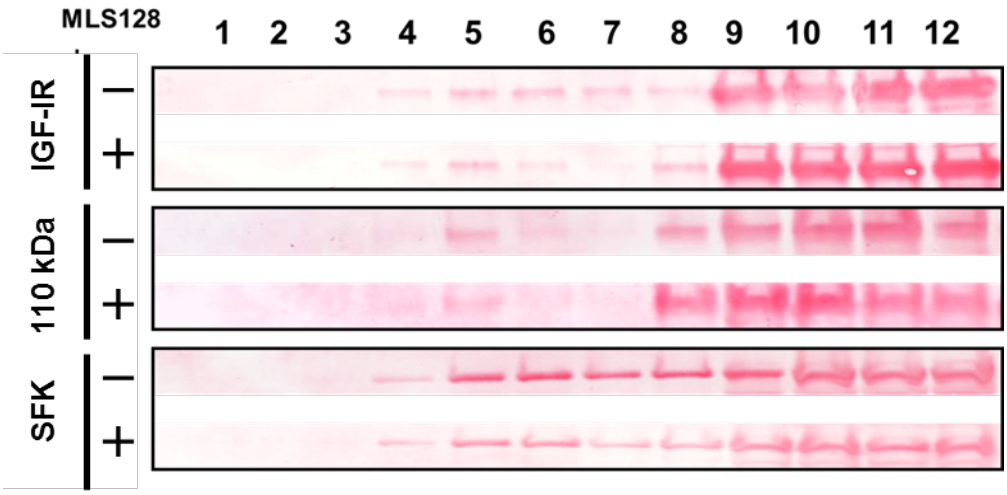

B LS180

Figure 22. Effects of MLS128 treatment on IGF-IR and 110 kDa GP in the microdomains of HT29 and LS180 cells.

Sucrose gradient fractionations of HT29 **(A)** and LS180 **(B)** cells that were treated with PBS (-MLS128) or MLS128 (+MLS128) were immunoblotted with anti-IGF-IR, MLS128, and anti-SFK antibodies.

3.5.5. Identification of 110 kDa GP

Extensive efforts have been made to identify the 110 kDa GP that was found to be the receptor for MLS128 in three colon cancer cell lines. It represents, after all, the first step in understanding the mechanisms by which MLS128 inhibits colon cancer cell growth. Figures 20-1 and 20-2 summarize results of two-dimensional gel electrophoresis of HT29 and LS180 cell lysates, respectively. Silver staining resulted in numerous proteins (Fig. 23-1 and 23-2 #1) whereas CBB staining depicted around 100 abundant proteins (Fig. 23-1 and 23-2 #2). Some of these were stained by MLS128 (Fig. 23-1 and 23-2 #3), indicating that Tn-antigen epitopes are present in quite a few proteins.

Spots depicting the candidate 110 kDa GP are indicated by arrows in Fig. 23-1 #3 and 23-2 #3. The position is identified by comparing the immunoblot of HT29 immunoprecipitates, which only revealed three MLS128-stainable spots in the area (Fig. 23-3 #1). In two-dimensional electrophoresis, the same glycoproteins with different numbers of sialic acid residues are most often separated on a scale with evenly spaced intervals by isoelectric focusing. Since 110 kDa GP is expected to contain clustered *O*-glycans based on its reactivity with MLS128, these three spots may represent the same protein with microheterogeneity of its glycans. In contrast, these spots of 110 kDa GP were not observed in the immunoprecipitates from LS180 cell lysate (Fig. 23-3 #2), although spots of 110 kDa were found in the lysate (indicated with an arrow in Fig. 23-2 #3). The reason why the spots seen in the HT29 cell lysate IP were not detected in the two-dimensional electrophoresis of LS180 cell lysate IP may be because of the difference in the density of Tn-antigen clusters on 110 kDa GP. A triplet Tn glycoepitope on the 110 kDa GP from LS180 cells might be less abundant than that of 110 kDa GP from HT29 cells. In IB, target molecules are immobilized on a membrane, allowing multivalent binding with antibodies, while they may have weaker interaction in solution in IP. This could cause a low recovery of 110 kDa GP in the immunoprecipitates from LS180 cell lysates.

To identify the 110 kDa proteins, the spots revealed by two-dimensional gel electrophoresis were subjected to in-gel digestion with trypsin. Tryptic peptides derived from these spots were then analyzed using matrix-assisted laser desorption ionization-time of flight (MALDI-TOF) mass spectrometry along with

software to search databases. Despite repeated attempts, the 110 kDa protein could not be successfully identified. This failure may be due to the 110 kDa GP's extremely low susceptibility to trypsin as a result of interference by abundant *O*-glycosylation, the lack of a database for glycosylated peptides, or the limited availability of samples.

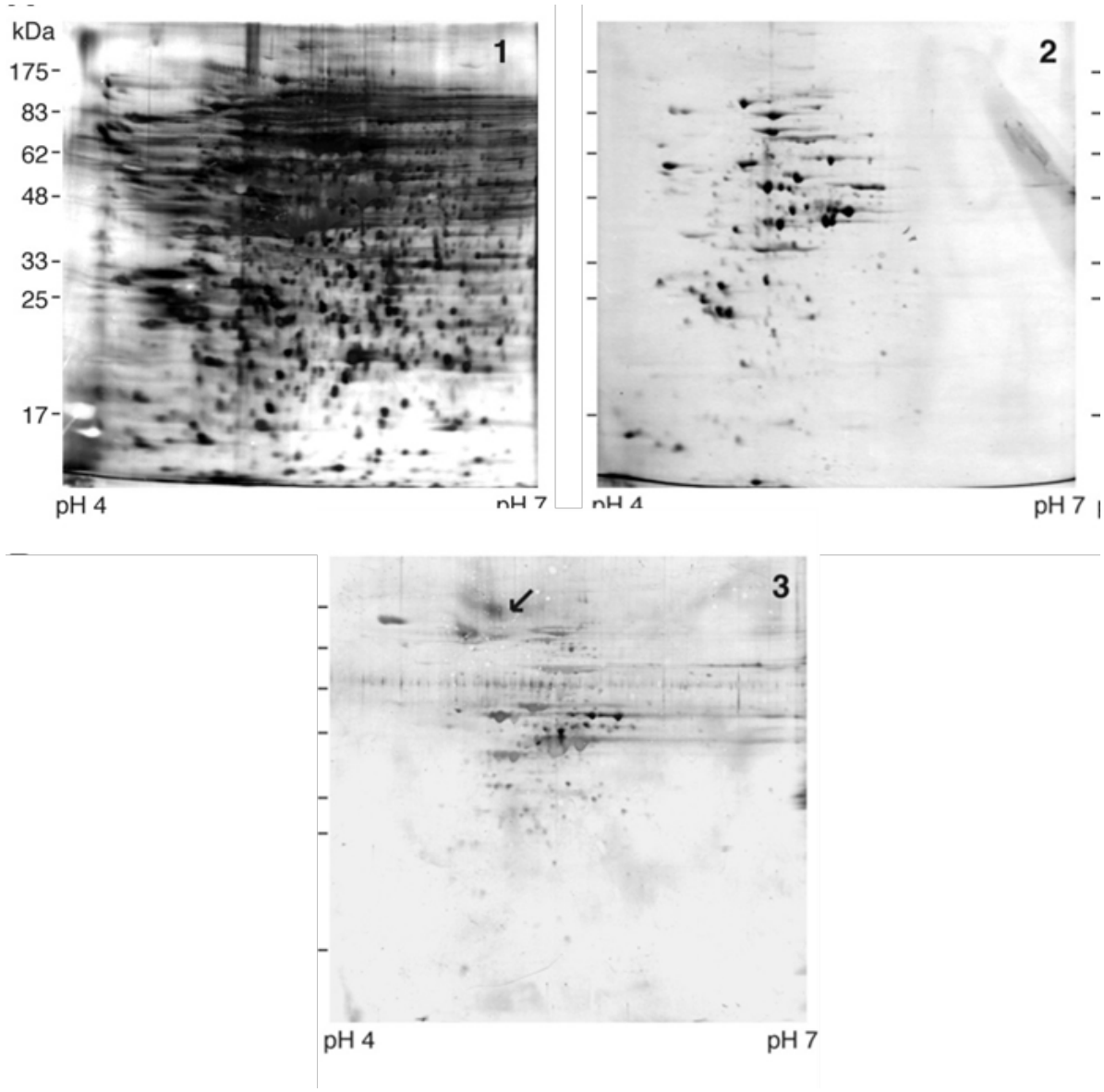

Figure 23-1. Two-dimensional gel electrophoresis of HT29 cell lysates.
Cell lysates prepared from HT29 were subjected to two-dimensional gel electrophoresis as described in the Methods. Silver staining (**1**), CBB staining (**2**), and IB with MLS128 (**3**) are shown. An arrow points to a spot indicating the possible location of 110 kDa GP in the immunoblots.

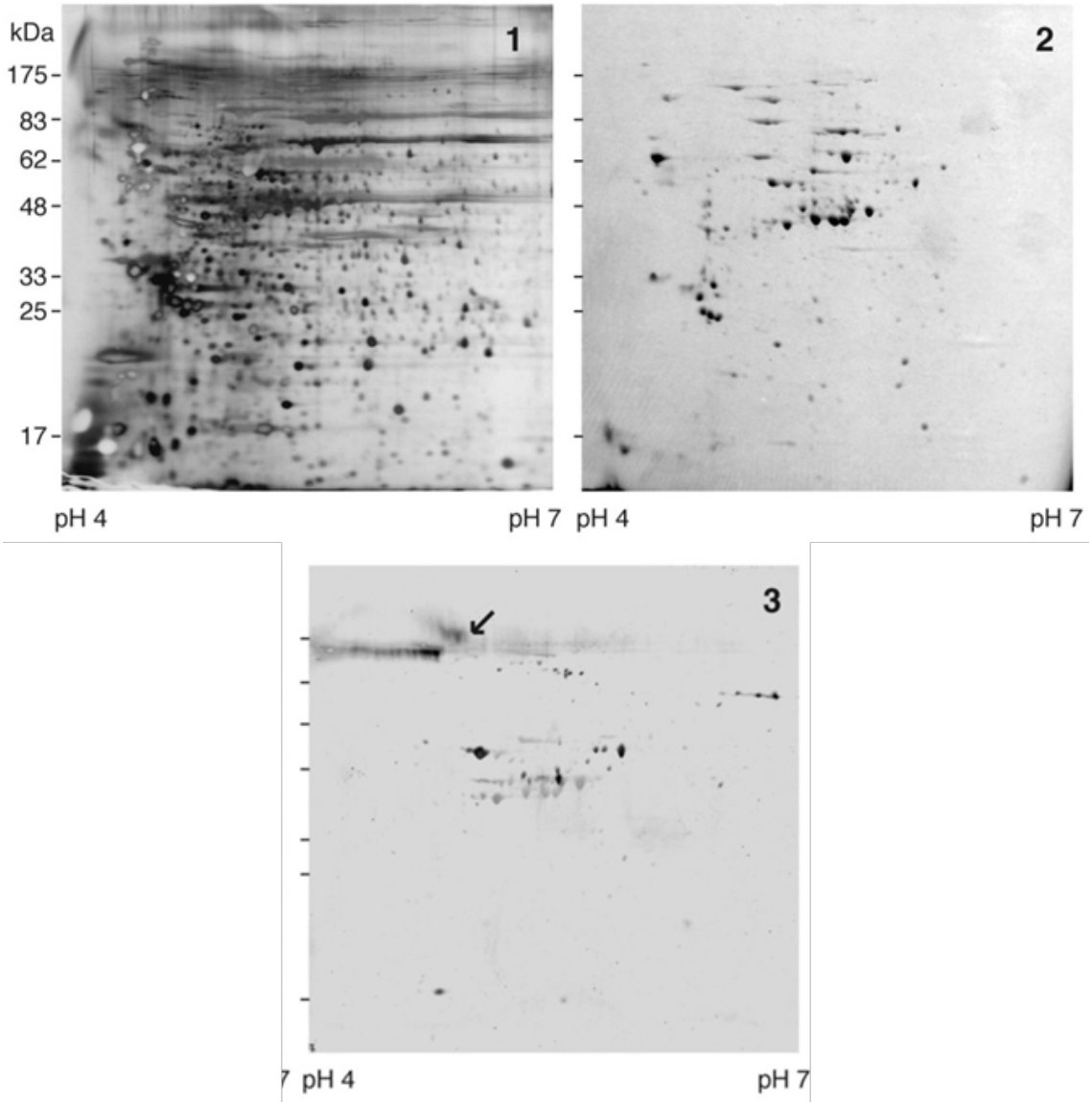

Figure 23-2. Two-dimensional gel electrophoresis of LS180 cell lysates.
Cell lysates prepared from LS180 were subjected to two-dimensional gel electrophoresis as described in the Methods. Silver staining (**1**), CBB staining (**2**), and IB with MLS128 (**3**) are shown. An arrow points to a spot indicating the possible location of 110 kDa GP in the immunoblots.

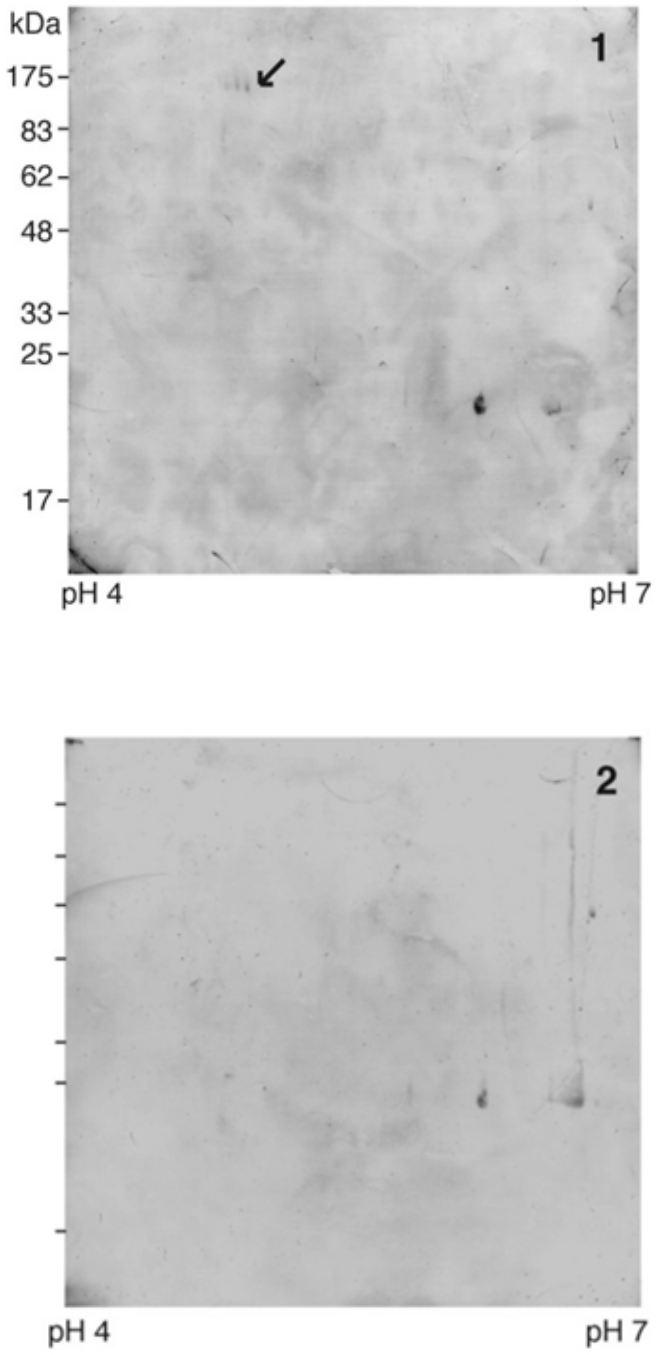

Figure 23-3. Two-dimensional gel electrophoresis of HT29 and LS180 immunoprecipitates. This figure shows results of two-dimensional gel electrophoresis of immunoprecipitates from HT29 lysates (1) and LS180 cell lysates (2) immunostained with MLS128. An arrow points to three spots in 1, indicating the location of 110 kDa GP in the immunoblots of HT29 and LS180 cell lysates (Fig. 23-1 #3 and Fig. 23-2 #3, respectively).

3.6 Discussion

The major question asked in this study was whether or not IGF-IR and 110 kDa GP are associated in HT29 cells. Given the results of IP/IB experiments, this possibility was excluded. Co-localization of IGF-IR and the MLS128 receptor in microdomains was, however, indicated by sucrose gradient centrifugation and IB using HT29 and LS180 cell lysates. A reduction in both receptors in microdomains was noted after HT29 and LS180 cells were treated with MLS128 for 3 days, which suggested that MLS128 binding to colon cancer cells resulted in modulation of signaling molecules associated with the microdomains. Whether or not the modulation of microdomain-associated signaling molecules plays a role in the ability of MLS128 to inhibit cancer cell growth remains to be answered.

Despite extensive efforts to identify the 110 kDa GP in HT29 and LS180 cell lysates and immunoprecipitates, this identification was unsuccessful. Two-dimensional electrophoresis and MLS128 IB revealed the heterogeneous nature of 110 kDa GP (Fig. 23-1 #3 and Fig. 23-2 #3). The three stained spots are characteristic of having a differing number of sialic acid residues on the same protein backbone. Identification of the 110 kDa protein was unsuccessful because of its microheterogeneity and extremely low susceptibility to trypsin due to its heavy glycosylation, both of which resulted in a low recovery of 110 kDa GP tryptic peptides. Methods of removing and purifying tryptic peptides from protein bands or spots on gels are sophisticated and well established. For mucin-type glycoproteins, however, trypsin digestion as is commonly used may not have worked efficiently due to abundant *O*-glycosylation, which would clearly render 110 kDa GP resistant to trypsin digestion. Procedures must be modified to optimize conditions for mucin-type glycoproteins in order to identify 110 kDa GP.

In summary, the current study provided new insights into the nature of 110 kDa GP. Although 110 kDa GP is not directly associated with IGF-IR, it is found in microdomains together with IGF-IR. MLS128 treatment may modulate receptors in microdomains. The 110 kDa GP was apparently heterogenous due to different degrees of its sialylation. Its heterogeneity and resistance to trypsin digestion

were apparently major obstacles to its successful identification.

In conclusion, a direct association between IGF-IR and 110 kDa GP can be ruled out as a possible mechanism for the inhibitory action of MLS128. The microdomain consists of a wide array of proteins, lipids, and receptors, and many signaling molecules are located in microdomains (Kabayama *et al.,* 2005, Oneyama *et al.,* 2009, Okamoto *et al.,* 1998). Sucrose gradient fractionation of HT29 and LS180 cell lysates was conducted with SFK as a marker, indicating that both IGF-IR and 110 kDa GP exist in microdomains (Fig. 21). IB results showed that MLS128 treatment resulted in the reduction in IGF-IR, 110 kDa GP, and SFK bands intensities (Fig. 22). This finding suggests that MLS128 modulates microdomains in some yet unknown manner.

The key to determining the inhibitory action of MLS128 lies in the 110 kDa GP since MLS128 bound to this GP on the surface of colon cancer cells and inhibited the growth of those cells. Two-dimensional gel electrophoresis was performed to identify 110 kDa GP, but so far efforts have been unsuccessful. This may be due to the fact that 110 kDa GP is highly insusceptible to trypsin or the result of interference by abundant O-glycosylation, the lack of a database for glycosylated peptides, or the limited availability of samples. Two-dimensional gel electrophoresis with IP from HT29 however, revealed three distinctive MLS-128 stainable spots (Fig. 23-3). In two-dimensional electrophoresis, the same GPs with different number of sialic acid residues are most often separated with evenly spaced intervals by isoelectric focusing. Since 110 kDa GP is expected to contain clustered O-glycans, these three spots may represents the same protein with microheterogeneity of its glycans. In contrast, those three spots were not detected in LS180, possibly because Tn antigen clusters on 110 kDa GP from LS180 are less dense than those in HT29, resulting in a low recovery of 110 kDa GP in the immunoprecipitate from LS180 cells. IB results of immunoprecipitates from both cells also indicated that the intensity of the 110 kDa band from HT29 cell lysates was stronger than that derived from LS180 cell lysates (data not shown). In order to successfully determine the identity of 110 kDa GP, methods have to be optimized to increase the recovery of 110 kDa GP.

Chapter 4

Limited proteolysis of the MLS128 binding proteins from LS180 and HT29 colon cancer cells

4.1 Summary

During characterization of HT29 cells using sucrose gradient fractionation (Chapter 3), an interesting phenomenon unexpectedly became apparent. Western blotting experiments were usually carried out immediately after sucrose gradient fractionation but were repeated after fractions had been stored frozen for 3-4 years.

IGF-IR blots done with the frozen fractions revealed that IGF-IR was still intact after 3 years of storage. In contrast, MLS128 immunoblots revealed the appearance of specific degradation products with molecular masses of 66 and 41 kDa, which add up to approximately 110 kDa, thus suggesting that a protease-susceptible region may exist in the middle of 110 kDa GP.

MLS128-stainable 46 kDa were observed in the microdomain fractions of LS180 cell lysates that had been frozen for 4 years.

This finding may support the notion that there are differences in the abundance and/or heterogeneity of *O*-glycosylation of the 110 kDa GP produced by HT29 or LS180 cells.

Different sizes found in microdomain-associated 110 kDa GPs from HT29 and LS180 cells may provide clues to help identify the 110 kDa GP.

4.2 Introduction

Proteolysis is the breakdown of proteins into smaller polypeptides or amino acids. This generally occurs as a result of the hydrolysis of the peptide bond, and is most commonly achieved by cellular enzymes called proteases, but it may also occur as a result of intramolecular digestion as well as by non-enzymatic methods, such as the action of mineral acids and heat. Proteolysis in organisms serves many purposes; for example, digestive enzymes break down proteins in food to provide amino acids for the organism, while proteolytic processing of the polypeptide chain after its synthesis may be necessary for the production of an active protein. Proteolysis is also important in the regulation of some physiological and cellular processes, as well as in preventing the accumulation of unwanted or abnormal proteins in cells. Proteins in cells are also constantly being broken down into amino acids. This intracellular degradation of protein serves a number of functions - it removes damaged and abnormal proteins and prevents their accumulation, and it also serves to regulate cellular processes by removing enzymes and regulatory proteins that are no longer needed. The amino acids may then be reused for protein synthesis.

Endopeptidases, or endoproteinases, are proteolytic peptidases that break the peptide bonds of nonterminal amino acids. Endopeptidases are categorized into five major classes: cysteine endopeptidases, aspartic endopeptidases, serine proteinases, metallo-endopeptidases, and threonine endopeptidases. The use of peptidase inhibitors is essential to preventing protein breakdown during preparation of cellular proteins, including GPs.

Several studies have reported protein degradation after a series of freeze-thaw cycles or even after purification. An example is a study by Kathuria *et al*.(1986), which revealed an intact 90-kDa β subunit of the human insulin receptor is degraded first to an 88-kDa form and then to a 50-kDa β_1-subunit form by proteolysis, even after purification, when stored at 4 ˚C. The current study found that 110kDa GP degradation occurred in frozen samples of sucrose gradient fractionations of HT29 and LS180 cell lysates.

This chapter summarizes the limited proteolysis noted during the microdomain experiments described in Chapter 3.

4.2 Materials

Production and characterization of MLS128 were as previously described in Chapter 1.

LS180 and HT29 human colon adenocarcinoma cells were obtained from the American Tissue Type Culture Collection.

Rabbit anti-IGFIRβ, and rabbit anti-β actin were purchased from Cell Signaling Technology (Beverly, MA, USA).

Rabbit anti-SFK (SRC 2; sc-18) was purchased from Santa Cruz Biotechnology (Santa Cruz, CA, USA).

Anti-rabbit or -mouse secondary antibody labeled with biotin was from Kirkegaard & Perry Laboratories (Gaithersburg, MD, USA).

Cell culture media (DMEM and McCoy's 5A) were purchased from Invitrogen (Carlsbad, CA).

4.4 Methods

Cell culture

LS180 cells were cultured in DMEM containing 10% fetal bovine serum (FBS) supplemented with 4.5 mg/mL D-glucose and 110 µg/mL pyruvic acid. HT29 cells were cultured in McCoy's 5A containing 10% FBS. All culture media included a 1% penicillin-streptomycin solution (Sigma-Aldrich).

Sucrose gradient fractionation of HT29 and LS180 cell lysates

All steps were carried out at 4°C. HT29 and LS180 cells grown in 3 - 5 150-mm dishes were washed with chilled PBS and lysed in 2 mL lysis buffer B (50 mM Tris–HCl, pH 7.4, 100 mM NaCl), containing protease inhibitors and 1 mM PMSF, 10 mM sodium vanadate, and 0.1 % NP40 on ice for 20 min. After centrifugation for 5 min at 1300 × g, supernatants (2 mL) were diluted with 2 mL of 85% (w/v) sucrose in 10 mM Tris-HCl, pH 7.5, containing 150 mM NaCl and 5 mM EDTA (TNE buffer). The diluted lysates were overlaid with 4 mL of 30% sucrose (w/v) and then with 4 mL of 5% sucrose (w/v) in TNE buffer in an ultracentrifuge tube. The samples were centrifuged at 39,000 rpm for 18 h in an SW41 rotor (Beckman Instruments, Palo Alto, CA), and fractions were collected from the top for IB analysis. Fractions were immunoblotted with anti-Src family kinase (SFK), which served as an internal marker for microdomains.

Western blotting

The fractions were separated by sodium dodecyl sulfate-polyacrylamide gel electrophoresis (SDS-PAGE) and transferred to polyvinylidene difluoride (PVDF) membranes. The membrane was blocked with 3% BSA in 50 mM Tris-HCl buffer, pH 7.4, containing 0.15 M NaCl and 1% Tween 20 (TBST) for 1 h at room temperature. Western blotting was carried out with anti-IGF-IR, anti-SFK, and MLS128 as primary antibodies. Bound primary antibodies were then detected with biotin-labeled secondary antibodies using a Vectastain ABC-Amp kit and an alkaline phosphatase kit (Vector Laboratories, Inc. Burlingame, CA, USA).

4.5 Results

4.5.1. A limited amount of microdomain-associated proteolysis of 110 kDa GP

During sucrose gradient fractionation of HT29 cells lysates and IB of fractions with MLS128, an interesting phenomenon unexpectedly became apparent. Western blotting experiments were usually carried out immediately after sucrose gradient fractionation (Fig. 24 A, C, and E). The results shown in Fig. 24 B, D, and F are, however, immunoblot experiments using the same fractions that had been kept frozen for 3-4 years.

IB with anti-IGF-IR as shown in Fig. 24 B (the same as Fig. 21 A) was repeated 3 years after fractionation since the background of the original immunoblot was too high to clearly identify the IGF-IR band in microdomains (Fig. 24 A). An IGF-IR blot that was redone with the frozen fractions revealed that IGF-IR is still intact after storage for 3 years (Fig. 24 B).

In contrast, an MLS128 immunoblot of frozen samples as shown in Fig. 24 D revealed degradation products with molecular masses of 66 and 41 kDa, which would add up to approximately 110 kDa, as seen in the immunoblot of fresh samples (Fig. 24 C, the same as Fig. 21 B). This finding suggested that a protease-susceptible region may exist in the middle of 110 kDa GP.

Figure 24 E and F shows experiments involving Western blot analyses of sucrose gradient-fractionated LS180 cell lysates that had been frozen for 4 years. Interestingly, the degradation products of an MLS128-stainable 46kDa band, with a different size than that of fragments derived from HT29 cell lysates, were observed in the microdomains of LS180 cell lysate fractions that had been frozen for 4 years (Fig. 24 F).

The aforementioned phenomena suggested that the 110 kDa GP became susceptible to microdomain-associated proteases during storage, freezing, and thawing.

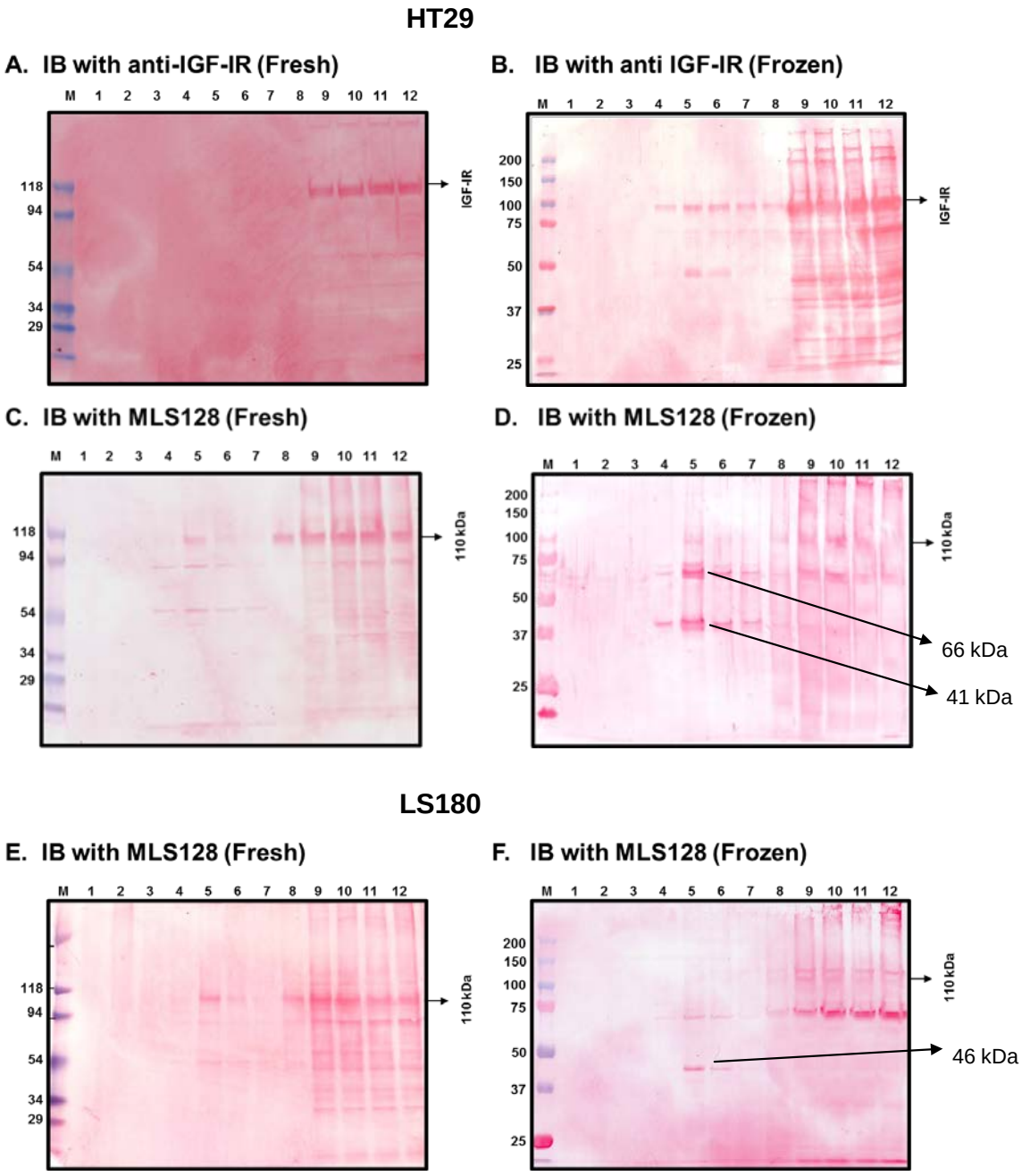

Figure 24. Comparison of immunoblots carried out using fresh and frozen fractions from HT29 (A-D) and LS180 cells (E-F).

IB of sucrose gradient-fractionated samples that were freshly prepared (A, C and E) and stored at –80 ºC for 3 or 4 years (B, D and F) are shown. Fractions 1-12 separated from cell lysates were immunoblotted with anti IGF-IR (A and B) and MLS128 (C-F).

4.5.2. Possible differences in the limited proteolysis of 110 kDa GP derived from two different colon cancer cell lines

To compare the degradation products from the microdomain-associated 110 kDa GP of HT29 and LS180 cells, fractions 5 and 6 from both microdomains that had been immunoblotted with MLS128 were compared in Fig. 25.

As the bands indicate, the molecular masses of the degradation products derived from HT29 and LS180 cells differ from 66/41 kDa to 46 kDa. Unlike the 110 kDa GP fragment of 66 kDa derived from HT29 cells, 70 kDa is seen in fractions 5 and 6 from LS180 cell lysates. In LS180 cell lysates, however, abundant 75 and 73 kDa proteins that are endogenous biotin-containing enzymes (Robinson *et al*. 1983) apparently interfered with this observation. IB using non-biotin involving color development indicated the presence of a 70 kDa fragment (data not shown).

These results suggest that a protease-susceptible region may exist in the middle of 110 kDa GP from both HT29 and LS180 cells. However, the different sizes observed in the two cell lines provide further information about the difference in the structure of 110 kDa GP in terms of its glycosylation sites and abundance.

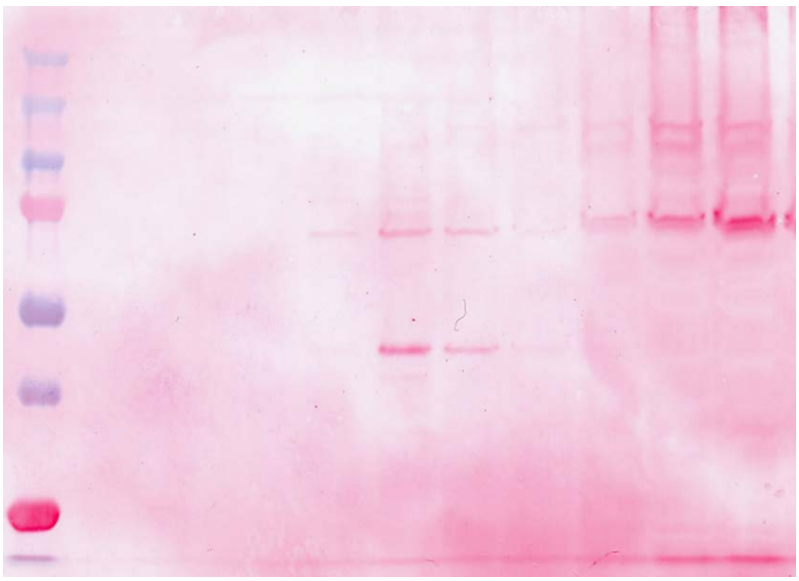

Figure 25: IB of frozen fractions 5-6 from HT29 and 5-10 from LS180 cells treated with MLS128.

Immunoblots shown in Fig. 24D and F are compared side by side. Degradation products from HT29 cells (66/41 kDa) and LS180 cells (46kDa) are clearly observed while the 70 kDa band from LS180 cell lysates cannot be definitely distinguished from endogenous biotin-containing enzymes (Robinson *et al.* 1983).

4.6 Discussion

An interesting finding is that limited proteolysis occurred in microdomain-associated 110 kDa GP after it was frozen and stored. Two independent observations involving HT29 and LS180 cells suggested the existence of protease-susceptible sites in the 110 kDa GP. The first was that microdomain-associated 110 kDa GP degraded into two fragments in HT29 cells; these fragments were 66 and 41 kDa, which add up to almost 110 kDa (Fig. 26, Hypothesis 1). Another possibility is that 110 kDa GP degrades into smaller fragments, first to 66 kDa and then to 41 kDa (Fig. 26, Hypothesis 2). The second observation was that 46 kDa fragments were produced in the microdomains derived from LS180 cell lysates stored at -80ºC. Results regarding 110 kDa degradation products are, however, inconclusive due to uncertainty about production of the 70 kDa fragment. This aspect needs to be investigated further. Although further confirmation is required, the likelihood is that the degradation products from both cell lines differ in size.

Since bands were generated from 110 kDa GP in cells that had not been treated with MLS128, conformational relaxation during storage, freezing, and thawing must have exposed the cleavage site(s) to contaminating proteases, resulting in limited proteolysis as was observed. Although protease inhibitor cocktails were added to cell lysates and during sucrose gradient fractionation, degradation of 110 kDa still occurred, which suggests that unidentified proteases that are resistant to the added inhibitors are responsible for the limited proteolysis of 110 kDa GP.

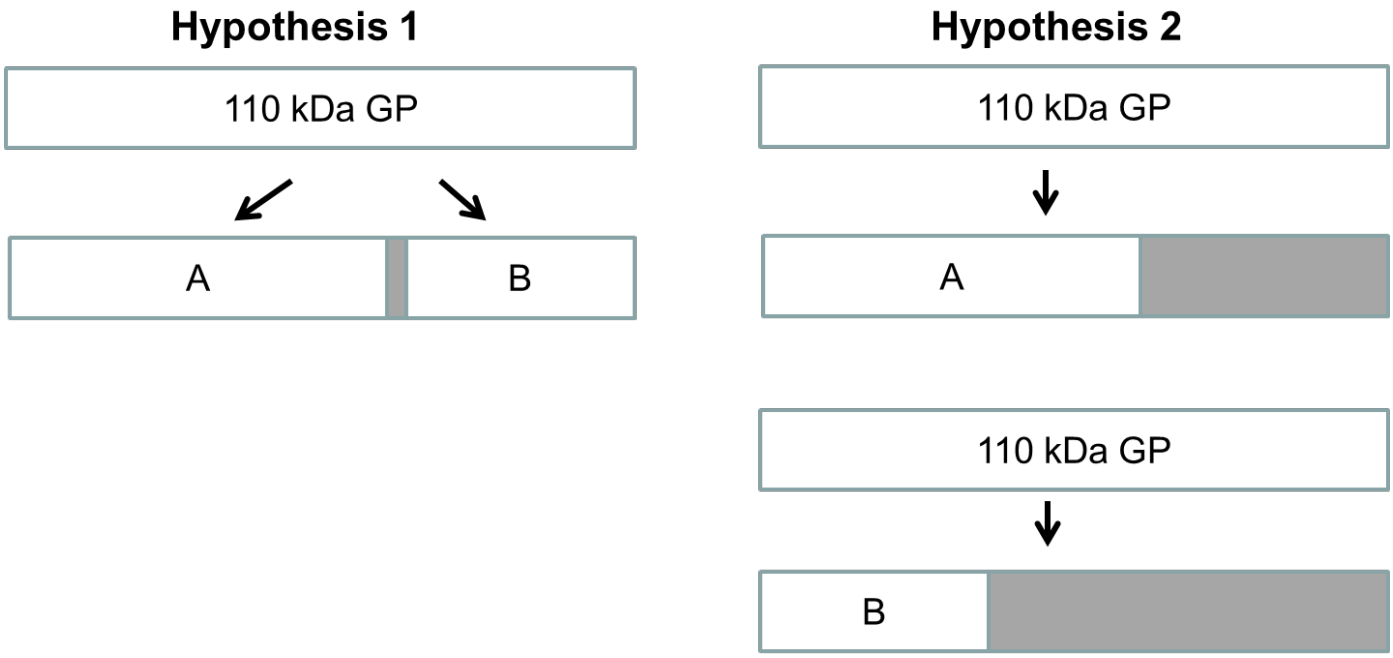

Figure 26: Diagram of possible degradation products from 110 kDa GP associated with microdomains of HT29 cell lysates.

Hypothesis 1: 110 kDa GP degraded into two smaller fragments A and B, i.e. 66 kDa and 41 kDa fragments, respectively.
Hypothesis 2: 110 kDa GP first degraded into a 66 kDa fragment (A) and then into 41 Da fragment (B).

The grey areas indicate a protease-susceptible domain or site where O-glycans are expected to be sparsely found.

Chapter 5

Conclusion

In tumor cells, glycoproteins are often abnormal, both in structure and quantity. Incomplete glycosylation is a frequent aspect of glycosylation alterations in cancer cells. Tn antigens are shielded by extended glycosylation in healthy and benign tissues but are uncovered in approximately 90 % of carcinomas (Springer, 1984, 1997). Since Tn antigen was first identified, it has been studied extensively as a cancer biomarker and it has been characterized as one of the most specific structures associated with cancer. Recent studies have shifted to investigating the Tn antigen as a potential target for cancer therapeutics. MLS128 is a monoclonal antibody that binds to two or three consecutive Tn antigens. A previous study revealed that MLS128 inhibits cancer cell growth and that IGF-IR down-regulation or signaling is a potential mechanism for its inhibitory action. In Chapters 2 and 3, anti-IGF-IR mAb 1H7 was used along with MLS128 to study their effects on colon cancer cells. The aim of this study was to investigate the mechanism of MLS128's inhibitory action and its possible interaction with IGF-IR signaling.

In Chapter 2, the effects of MLS128 and 1H7 mAbs on three colon cancer lines - HT29, LS180, and LS174T - were investigated. Results showed that the growth of all three colon cancer cell lines was inhibited to a certain degree after treatment with both mAbs.

This study demonstrated that the growth of colon cancer cells is IGF-I dependent. Inhibition of growth by 1H7 was only 60% (Fig. 9, Chapter 2), suggesting that there must be other growth signaling pathways involved in colon cancer cell growth besides IGF-IR signaling. IGF-IR activated downstream signaling via Akt and MAPK phosphorylation in colon cancer cells. MLS128 did not affect IGF-IR signaling.

IGF-IR was significantly down-regulated by 1H7 treatment in all three colon cancer cell lines. That down-regulation was most significant in HT29 cells.

MLS128 treatment caused the partial disappearance of 110 kDa GP in all three cancer cell lines. This effect was most significant in HT29 cells. MLS128 did not, however, appear to affect IGF-IR levels except in HT29 cells cultured for 3 days (Figs. 14 and 15, Chapter 2)

Although IGF-IR down-regulation and signaling may not be the main mechanism for the inhibitory action of MS128, the possibility of a physical association between IGF-IR and 110 kDa GP still remained. As described in Chapter 3, however, no direct association between IGF-IR and 110 kDa GP was noted.

A wide array of proteins, lipids, receptors, and many signaling molecules are located in microdomains (Okamoto *et al.,* 1998, Kabayama *et al.,* 2005, Oneyama *et al.,* 2009). In Chapter 3, possible co-localization of IGF-IR and 110 kDa in microdomains was investigated. Both IGF-IR and 110 kDa were found in microdomains (Fig. 21, Chapter 3). MLS128 treatment resulted in a reduction in IGF-IR, 110 kDa GP, and SFK localized in microdomains (Fig. 22, Chapter 3), suggesting that MLS128 may modulate microdomains via an as-yet-unidentified mechanism.

MLS128 bound to 110 kDa GP in colon cancer cells, thereby inhibiting cell growth. The 110 kDa GP must be identified to understand the inhibitory action of MLS128 on colon cancer cells. Two-dimensional gel electrophoresis was performed to identify 110 kDa GP, but no candidate glycoprotein has been found thus far. This may be due to the fact that 110 kDa GP is highly insusceptible to trypsin or the result of interference by abundant O-glycosylation, the lack of a database for glycosylated peptides, or the limited availability of samples.

Two-dimensional gel electrophoresis with IP from HT29 cell lysates, however, showed three distinctive MLS-128 stainable spots (Fig. 23-3, Chapter 3). In two-dimensional electrophoresis, the same GPs with different number of sialic acid residues are most often separated with evenly spaced intervals by isoelectric focusing. Since 110 kDa GP is expected to contain clustered O-glycans, these three spots may represent the same protein with microheterogeneity of its glycans. In contrast, those three spots were not detected in IP from LS180 cell lysates. This may be explained by differences in Tn antigen clusters on 110 kDa GP. If Tn antigens on 110 kDa GP derived from LS180 cells are less dense than those on 110 kDa GP derived from HT29 cells, IP with MLS128 would result in a low recovery of 110 kDa GP from LS180 cells. In order to successfully identify 110 kDa GP, methods have to be improved to increase recovery of 110 kDa GP and its peptides.

An important finding from this study is the limited proteolysis of 110 kDa GP that was observed in microdomain fractions frozen for several years. Observations with both HT29 and LS180 cells suggested the existence of protease-susceptible sites in the 110 kDa GP. Conformational relaxation during storage, freezing, and thawing must have exposed the cleavage site(s) to contaminating proteases, resulting in limited proteolysis as was observed. Although protease inhibitor cocktails were added to cell lysates and during sucrose gradient fractionation, degradation of 110 kDa still occurred, suggesting that unidentified proteases that are resistant to the added inhibitors are responsible for the limited proteolysis of 110 kDa GP. This observation of limited proteolysis should help identify 110 kDa and ultimately uncover the mechanism by which MLS128 inhibits colon cancer cell growth.

Returning to the hypothesis that was initially proposed, the current findings have ruled out the possibility that IGF-IR signaling, down-regulation, and its direct association with 110 kDa GP are the main mechanisms by which MLS128 inhibits the growth of colon cancer cells.

One of the significant findings to emerge from this study is that colon cancer growth is IGF-IR-dependent. Another is evidence of the inhibition of cell growth and IGF-IR down-regulation after treatment with 1H7.

Although the inhibitory mechanism of MLS128 has yet to be determined and 110 kDa GP still needs to be identified, this research provides several hints and insights for future studies to reach those goals.

REFERENCES

Ando H, Matsushita T, Wakitani M, Sato T, Kodama-Nishida S, Shibata K, Shitara K, Ohta S. **Mouse-human chimeric anti-Tn IgG1 induced anti-tumor activity against Jurkat cells in vitro and in vivo.** Biol. Pharm. Bull. 2008;31:1739-1744.

Baserga R, Hongo A, Rubini M, Prisco M, Valentinis B. **The IGF-I receptor in cell growth, transformation and apoptosis**. Biochim Biophys Acta. 1997; 1332: F105-F126.

Butler A.A., Yakar S., Gewolb IH., Karas M., Okubo Y., LeRoith D. **Insulin-like growth factor-I receptor signal transduction: at the interface between physiology and cell biology**. Comparative Biochemistry and Physiology, Part B 1998; 121(1): 19–26

Cancer Genome Atlas Network. **Comprehensive molecular characterization of human colon and rectal cancer**. Nature 2012, 487: 330-337.

Charpin C, Pancino G, Osinaga E, Bonnier P, Lavaut MN, Allasia C, Roseto A. **Monoclonal antibody 83D4 immunoreactivity in human tissues: cellular distribution and microcytophotometric analysis of immunoprecipitates on tissue sections.** Anticancer Res. Jan-Feb 1992; 12(1): 209-23.

Claus-Henning K. and Heinz-Josef L. **Chemotherapy with targeted agents for the treatment of metastatic colorectal cancer.** Oncologist 2009, 14:478-488.

Fujita-Yamaguchi Y**. Renewed interest in basic and applied research involving monoclonal antibodies against an oncofetal Tn-antigen.** J Biochem. 2013; 152: 103-105.

Freire T., Osinaga E. **Immunological and biomedical relevance of the Tn-antigen.** Immunologia Jan-Mar 2003; 22(1): 27-38.

Hang HC, and Bertozzi CR. **The chemistry and biology of mucin-type O-linked glycosylation. Bioorganic & Medicinal Chemistry** 2005; 13: 5021–5034.

Itzkowitz SH, Mei Yuan, Montgomery CK, Kjeldsen T., Takahashi HK, Bigbee WL, and Kim YS. **Expression of Tn, sialosyl-Tn, and T antigens in human colon cancer.** Cancer Res 1989; 49: 197-204.

Itzkowitz SH, Bloom EJ, Lau TS, Kim YS. **Mucin associated Tn and sialosyl-Tn antigen expression in colorectal polyps.** Gut 1992; 33: 518–23.

Kathuria S. Hartman S, Grunfeld C, Ramachandran J, and Fujita-Yamaguchi Y. **Differential sensitivity of two functions of the insulin receptor to the associated proteolysis: Kinase action and hormone binding**. Proc Natl Acad Sci USA, 1986; 83:8570-8574.

Kabayama K, Sato T, Kitamura F, Uemura S, Kang B.W, Igarashi Y, Inokuchi J. **TNF alpha-induced insulin resistance in adipocytes as a membrane microdomain disorder: involvement of ganglioside GM3.** Glycobiology 2005; 15: 21–29.

Kubota T, Matsushita T, Niwa R, Kumagai I, Nakamura K. **Novel anti-Tn single-chain Fv-Fc fusion proteins derived from immunized phage library and antibody Fc domain.** Anticancer Res. 2010;30:3397-3405.

Larsson O, Girnita A, Girnita L. **Role of insulin-like growth factor 1 receptor signaling in cancer.** Br J Cancer 2005; 92: 2097-2101.

LeRoith D, Werner H, Beitner-Johnson D, Roberts CT Jr. **Molecular and cellular aspects of the insulin-like growth factor I receptor.** Endocr Rev. 1995; 16: 143-163.

Li SL, Kato J, Paz IB, Kasuya J, Fujita-Yamaguchi Y. **Two new monoclonal antibodies against the α subunit of the human insulin-like growth factor-I receptor.** Biochem Biophys Res Commun. 1993; 196: 92-98.

Li SL, Liang SJ, Guo N, Wu AM, Fujita-Yamaguchi Y. **Single-chain antibodies against human insulin-like growth factor I receptor: Expression, purification, and effect on tumor growth.** Cancer Immunol Immunother. 2000; 49: 243-252.

Matsumoto-Takasaki A, Hanashima S, Aoki A, Yuasa N, Ogawa H, Sato R, Kawakami H, Mizuno M, Nakada H, Yamaguchi Y, and Fujita-Yamaguchi Y. **Surface plasmon resonance and NMR analyses of anti Tn-antigen MLS128 monoclonal antibody binding to two or three consecutive Tn-antigen clusters.** J. Biochem. 2012; 151, 273-282

Miller BS, Yee D. **Type I insulin-like growth factor receptor as a therapeutic target in cancer.** Cancer Res. 2005; 65: 10123-10127.

Mikami K, Yamaguchi D, Tateno H, Hu D, Qin S, Kawasaki N, Yamada M, Matsumoto N, Hirabayashi J, Ito Y, Yamamoto K. **The sugar-binding ability of human OS-9 and its involvement in ER-associated degradation**. Glycobiology. 2010; 20, 310-321.

Morita N, Yajima Y, Asanuma H, Nakada H, Fujita- Yamaguchi Y**. Inhibition of cancer cell growth by anti-Tn monoclonal antibody MLS128**. Biosci Trends. 2009; 3: 32-37.

Nakada H, Numata Y, Inoue M, Tanaka N, Kitagawa H, Funakoshi I, Fukui S, and Yamashina I. **Elucidation of an essential structure recognized by an anti-GalNAc alpha-Ser(Thr) monoclonal antibody (MLS 128).** J. Biol. Chem. 1991; 266, 12402-12405

Nakada H, Inoue M, Numata Y, Tanaka N, Funakoshi I, Fukui S, Mellors A, Yamashina I. **Epitopic structure of Tn glycophorin A for an anti-Tn antibody (MLS128).** Proc Natl Acad Sci USA. 1993; 90: 2495-2499.

Numata Y, Nakada H, Fukui S, Kitagawa H, Ozaki K, Inoue M, Kawasaki T, Funakoshi I, Yamashina I. **A monoclonal antibody directed to Tn antigen**. Biochem Biophys Res Commun. 1990; 170:981-985.

Okamoto T, Schlegel A, Scherer PE, Lisanti MP. **Caveolins, a family of scaffolding proteins for organizing "preassembled signaling complexes" at the plasma membrane.** J Biol Chem. 1998; 273, 5419-5422.

Oneyama C, Iino T, Saito K, Suzuki K, Ogawa A, Okada M. **Transforming potential of Src family kinases is limited by the cholesterol-enriched membrane microdomain.** Mol Cell Biol. 2009; 29: 6462-6472.

Oppezzo P, Osinaga E, Tello D, Bay S, Cantacuzene D, Irigoín F, Ferreira A, Roseto A, Cayota A, Alzari P, Pritsch O. **Production and functional characterization of two mouse/human chimeric antibodies with specificity for the tumor-associated Tn-antigen.** Hybridoma 2000;19:229-239.

Osinaga E, Bay S, Tello D, Babino A, Pritsch O, Assemat K, Cantacuzene D, Nakada H, and Alzari P**. Analysis of the fine specificity of Tn-binding proteins using synthetic glycopeptide epitopes and a biosensor based on surface plasmon resonance spectroscopy.** FEBS Lett. 2000; 469: 24-28

Pancino, G.F., Osinaga, E., Vorauher, W., Kakouche, A., Mistro, D., Charpin, C., and Roseto, A**. Production of a monoclonal antibody as immunohistochemical marker on paraffin embedded tissues using a new immunization method**. Hybridoma 1990; 9(4): 389-395.

Pollak MN, Schernhammer ES, Hankinson SE. **Insulin-like growth factors and neoplasia.** Nat Rev Cancer. 2004; 4: 505-518.

Reis CA, Sorensen T, Mandel U, et al. **Development and characterization of an antibody directed to an alpha-N-acetyl-D-galactosamine glycosylated MUC2 peptide.** Glycoconj J 1998; 15: 51–62.

Robinson BH, Oei J, Saunders M, Gravel R. **[^{3}H]biotin-labeled proteins in cultured human skin fibroblasts from patients with pyruvate carboxylase deficiency.** J Biol Chem. 1983; 247: 6660-6664.

Sachdev D, Li SL, Hartell JS, Fujita-Yamaguchi Y, Miller JS, Yee D**. A chimeric humanized single-chain antibody against the type I insulin-like growth**

factor (IGF) receptor renders breast cancer cells refractory to the mitogenic effects of IGF-I. Cancer Res. 2003; 63: 627-635.

Singh R, Subramanian S, Rhodes JM, Campbell BJ**. Peanut lectin stimulates proliferation of colon cancer cells by interaction with glycosylated CD44v6 isoforms and consequential activation of c-Met and MAPK: Functional implications for disease-associated glycosylation changes.** Glycobiology. 2006; 16: 594-601.

Springer G.F. **T and Tn, general carcinoma autoantigens.** Science. 1984; 224, 1198-1206.

Springer GF, Desai PR, Ghazizadeh M, Tegtmeyer H. **T/Tn pancarcinoma autoantigens: fundamental, diagnostic, and prognostic aspects.** Cancer Detect Prev 1995; 19: 173–82.

Springer GF. **Immunoreactive T and Tn epitopes in cancer diagnosis, prognosis, and immunotherapy.** J Mol Med 1997; 75: 594–602.

Takahashi H.K, Metoki R, and Hakomori S**. Immunoglobulin G3 monoclonal antibody directed to Tn antigen (tumor-associated alpha-N-acetylgalactosaminyl epitope) that does not cross-react with blood group A antigen.** Cancer Res. 1988; 48, 4361-4367.

Valentinis B., Baserga R. **IGF-I receptor signalling in transformation and differentiation.** J Clin Pathol: Mol Pathol 2001; 54: 133–137.

Varki A, Cummings R, Esko J, Freeze H, Stanley P, Bertozzi C, Hart G, Etzler M eds. **Essentials of Glycobiology, 2nd ed.** Cold Spring Harbor Laboratory Press 2009.

Welinder C, Baldetorp B, Borrebaeck C, Fredlund BM, and Jansson B. **A new murine IgG1 anti-Tn monoclonal antibody with in vivo anti-tumor activity.** Glycobiology 2011; 21(8): 1097–1107.

Ye JJ, Liang SJ, Guo N, Li SL, Wu AM, Giannini S, Sachdev D, Yee D, Brünner N,

Ikle D, Fujita-Yamaguchi Y. **Combined effects of tamoxifen and a chimeric humanized single chain antibody against the type I IGF receptor on breast tumor growth in vivo**. Horm Metab Res. 2003; 35:836-842.

Yee D. **Targeting insulin-like growth factor pathways**. Brit J Cancer 2006; 94: 465 – 468.

Yuasa N, Ogawa H, Koizumi T, Tsukamoto K, Matsumoto-Takasaki A, Asanuma H, Nakada H, and Fujita-Yamaguchi Y. **Construction and expression of anti-Tn antigen-specific single-chain antibody genes from hybridoma producing MLS128 monoclonal antibody.** J. Biochem. 2012; 151: 371-381.

Zamri N, Masuda N, Oura F, Yajima Y, Nakada H, Fujita-Yamaguchi Y. **Effects of two monoclonal antibodies, MLS128 against Tn-antigen and 1H7 against insulin-like growth factor-I receptor, on the growth of colon cancer cells.** BioSci Trends. 2012; 6(6):303-312.

Zeng Z, Weiser MR, D'Alessio M, Grace A, Shia J, Paty PB. **Immunoblot analysis of c-Met expression in human colorectal cancer: Overexpression is associated with advanced stage cancer.** Clin Exp Metastasis. 2004; 21:409-417.

Zhang Y, Zhang Y. **Growth inhibition of insulin-like growth factor I receptor monoclonal antibody to human colorectal cancer cells**. Cancer Invest. 2008; 26:230-236.

ACKNOWLEDGEMENTS

بسم الله الرحمن الرحيم

The author wishes to first thank Allah the most Gracious, the most Merciful.

This thesis would not have been possible without the cooperation and the help of individuals and organizations that have, in one way or another, contributed to and provided their valuable assistance during the preparation and completion of this study. The author wishes to express her sincerest gratitude to all of these individuals and organizations.

The author wishes to thank Professor Yoko Fujita-Yamaguchi, whose encouragement, guidance, and vast knowledge as an advisor helped to make this thesis possible.

The author wishes to thank Dr. Yukiko Yajima, who has been a great mentor providing unceasing support and help along the way.

The author wishes to thank all of the professors and personnel from the Dept. of Applied Biochemistry, Tokai University for their cooperation and help in various forms throughout this study.

The author wishes to thank Fumie Oura, Masuda Naoya, and other members of the Yamaguchi Laboratory for their friendship, cooperation, and support in bringing this study to fruition.

The author wishes to thank family members for their understanding, love, and support. The author's parents, Zamri Hassan and Zaharah Yahaya, have been a great source of motivation and strength.

The author wishes to thank fellow members of the Aspiring Malaysian Rijal for their friendship and time that made the author's time in Japan a meaningful one.

The author wishes to thank the Government of Malaysia for financial support through the Ministry of Higher Education (MOHE), as well as the Universiti Malaysia Pahang (UMP) for its support and encouragement of further study.

Thanks are extended to everyone who contributed to and assisted with the completion of this thesis, in one way or another. Hopes are that this thesis directly benefits others or possibly helps to motivate later researchers.